Fluid Dynamics &
Materials Processing

Tech Science Press

http://doi.org/10.32604/fdmp.2026.079861

REVIEW

A Review of Artificial Intelligence in Boiling Heat Transfer: Predictive Modeling, Dynamic Characterization, and Methodological Advances

Wei-Chen Tang, Xin Chen and Fei Dong*

Jiangsu University, School of Automotive and Traffic Engineering, 301 Xuefu Road, Zhenjiang, China
*Corresponding Author: Fei Dong. Email: jsdxdf@163.com

Received: 29 January 2026; Accepted: 26 March 2026; Published: 07 May 2026

ABSTRACT: Boiling heat transfer remains a cornerstone of efficient thermal management, with far-reaching implications for energy systems and industrial processes. Advances in this field not only deepen fundamental scientific understanding but also enable transformative improvements in energy efficiency, equipment performance, and operational safety. Contemporary research in this area focuses on accurate parameter prediction, intelligent image analysis, and quantitative characterization of bubble dynamics, collectively advancing both mechanistic insight and engineering optimization. In this context, artificial intelligence (AI), encompassing machine learning and deep learning techniques, has emerged as a powerful paradigm, offering significant advantages in predictive accuracy, data-driven analysis, and experimental efficiency. This paper provides a systematic review of AI applications in boiling heat transfer research. First, conventional approaches are critically assessed, highlighting the growing relevance and advantages of AI-based methodologies. Next, key machine learning algorithms are introduced and classified according to their roles and capabilities. Subsequently, recent advances in AI-driven prediction of heat transfer parameters, automated analysis of bubble dynamics, and the development of novel research methodologies are comprehensively examined. Finally, current achievements are synthesized, and future research directions are outlined, with particular emphasis on the integration of AI into real-time control and edge-computing frameworks for industrial thermal management.

KEYWORDS: Artificial intelligence; boiling heat transfer; bubble dynamics

1 Introduction

For decades, heat transfer research has remained a focal point in both academic and industrial circles, exerting profound impacts on enhancing energy utilization efficiency and equipment performance [1–4]. Boiling heat transfer, as one of the most extensively studied and widely utilized processes, represents a core domain in multiphase flow heat transfer research and holds pivotal significance in contemporary technological development [5,6]. This technology has been deeply integrated into multiple critical fields including aerospace technology, energy engineering, electronics, and industrial manufacturing, where heat transfer research plays an indispensable role.

Research on boiling heat transfer primarily encompasses the prediction of key parameters (including Critical Heat Flux and Heat Transfer Coefficient), the detection and analysis of boiling heat transfer images, and the calculation of bubble dynamics parameters. Traditional approaches for investigating boiling heat transfer mechanisms and bubble dynamics primarily rely on direct experimental measurements and numerical simulation techniques. Experimental methods enable direct observation of boiling phenomena

and acquisition of first-hand data, offering high reliability and intuitiveness, which establishes them as the benchmark for validating other research methodologies. However, these methods suffer from several limitations, including high costs, operational complexity, uncontrollable errors, and testing difficulties under specific conditions. Moreover, the experimental results often lack generalizability for deriving universal correlations [7,8]. In contrast, numerical simulation offers cost advantages and flexibility in simulating diverse operating conditions, while providing complete evolution data of key parameters (temperature, pressure, and velocity fields) during boiling processes. However, due to the inherent complexity and stochastic nature of boiling phenomena, such simulations are typically limited to simple geometric configurations, with their accuracy and reliability heavily dependent on both the precision of mathematical models and the rationality of boundary conditions [9,10]. Reference [10] systematically discusses the design and operational challenges of inlets for rocket-based combined cycle engines, emphasizing that the reliability of numerical simulations depends critically on accurately modeling boundary conditions and flow interactions.

With the rapid advancement of big data technologies and artificial intelligence algorithms, an increasing number of researchers are exploring AI applications in boiling heat transfer and bubble dynamics research. As this review will demonstrate, AI has demonstrated exceptional performance not only in predicting heat transfer coefficients, intelligent image recognition, and precise calculation of bubble dynamics parameters, but also in effectively optimizing traditional research methods such as soft sensors that infer hard-to-measure boiling parameters from readily available process variables, and numerical simulations. Consequently, researchers have developed various intelligent prediction models based on deep learning and machine learning algorithms, providing innovative approaches to revolutionize conventional research methodologies. Traditional AI models are characterized by simplicity and strong interpretability, primarily including machine learning (Support Vector Machine [11–13], Artificial Neural Network [14–16]), empirically-derived correlations from experimental data, physics-guided hybrid models, and shallow learning algorithms (K-Nearest Neighbor [17,18], Gaussian Process Regression [19,20]). These approaches are particularly suitable for small-scale datasets and simple tasks, and have been widely applied in Critical Heat Flux and Heat Transfer Coefficient prediction as well as bubble dynamics optimization studies. While demonstrating improved computational efficiency and prediction accuracy compared to conventional experimental and numerical methods, these models are constrained by their reliance on single databases or artificially synthesized pseudo-data. This limitation often leads to prevalent overfitting issues and limited applicability to real-world industrial problems. For instance, Poletaev et al. [8] demonstrated that traditional correlation-based methods for bubble recognition in two-phase flows performed poorly when bubbles overlapped or deviated from circular shapes—common occurrences in real experiments. By training neural networks on synthetically generated images that closely mimicked real experimental conditions, they achieved a 6–8 fold increase in processing speed and detected twice as many bubbles as conventional methods. This example powerfully illustrates how reliance on limited or idealized data can undermine model performance, and how carefully designed synthetic data can overcome such limitations. Modern AI models are characterized by high complexity and enhanced data processing capabilities, encompassing deep learning (Convolutional Neural Network [21–23], Graph Neural Network [24–26]), physics-informed neural networks [27–29], ensemble learning (Random Forest [30,31], Extreme Gradient Boosting [32,33]), transfer learning frameworks, and explainable AI [34,35]. These advanced models excel in handling large-scale datasets and complex tasks, delivering superior prediction accuracy, process optimization, and cross-scenario adaptability. Although requiring more sophisticated development processes, they demonstrate marked improvements in computational efficiency and application scope. Notably, these next-generation models

can extrapolate beyond experimental data limitations and address complex multiphysics coupling problems across diverse operating conditions, demonstrating enhanced reliability and practical applicability in engineering contexts.

A comprehensive understanding of AI models in boiling heat transfer research holds significant theoretical and practical value for elucidating heat transfer mechanisms, analyzing bubble dynamics, optimizing thermal performance, and developing high-efficiency enhancement technologies.

This paper systematically reviews recent advancements in AI applications for boiling research. To move beyond a mere catalog of techniques, we organize the literature through a Tri-Phase Validation System that maps AI developments onto three progressive stages:

Phase I: Foundational Models—establishing ML/DL baselines for tasks such as CHF/HTC prediction and bubble segmentation;

Phase II: Methodological Innovation—developing advanced architectures tailored to boiling-specific challenges (e.g., Transformers for parameter interactions, PINNs for physics embedding);

Phase III: Industrial Adaptation—translating these advances toward practical deployment through soft sensors, AI-accelerated numerics, and synergy with surface engineering.

This framework, applied throughout Sections 3–5, provides a structured lens for analyzing how the field has evolved. In contrast to recent reviews that primarily catalog AI techniques in thermal sciences—such as Chu et al. [36] focusing on machine learning applications for boiling parameter prediction, and Yang et al. [37] reviewing computer vision and machine learning methods for microchannel flow visualization and pattern recognition—the present work offers three distinct contributions: (i) a task-oriented taxonomy that links specific AI architectures to the physical nature of boiling problems; (ii) a critical assessment of methodological trade-offs, including accuracy versus interpretability, overfitting risks, and the role of physics-informed constraints; and (iii) organization through the Tri-Phase framework, which reveals not just what has been done but the trajectory of the field—from foundational proofs-of-concept through methodological refinement toward industrial application.

Accordingly, we first overview representative AI models and their distinctive features in Section 2. Second, we detail specific applications across three key areas: boiling heat transfer prediction in Section 3, bubble dynamics characterization in Section 4, and methodological innovations including soft sensors and numerical simulation enhancement in Section 5. Finally, we summarize current achievements, identify limitations, and propose future research directions in Section 6.

2 Categorization of Artificial Intelligence

Within the AI technology framework, machine learning and deep learning constitute two core branches that achieve intelligent tasks through data-driven methods and multi-layer neural network architectures, respectively. These approaches have not only enhanced the efficiency and precision of boiling heat transfer research but also provided innovative methodologies for addressing complex engineering challenges. This section introduces and analyzes current mainstream AI algorithms and their applications in boiling heat transfer research.

2.1 Machine Learning (ML)

ML is a data-driven technology that enables autonomous learning and optimization through statistical analysis and algorithmic modeling. At its core, ML extracts patterns from data to facilitate prediction and decision-making, with broad applications spanning image recognition, speech processing, intelligent

recommendation systems, and beyond. The following summarizes representative ML algorithms and their applications in boiling heat transfer research.

2.1.1 Supervised Learning (SL)

SL trains models on datasets with known input-output relationships to achieve accurate predictions for unseen data. These algorithms are particularly valuable for developing surrogate models that leverage historical or sample data to approximate complex numerical simulations, thereby significantly reducing computational frequency, shortening calculation cycles, and lowering operational costs. As illustrated in Fig. 1a [38], representative SL algorithms include radial basis function (RBF) models, support vector machine (SVM) models, and artificial neural networks (ANNs) [39]. Among these approaches, SVM has gained extensive application in boiling heat transfer research due to its unique advantages.

As a classical supervised learning algorithm, SVM demonstrates outstanding performance in handling small-sample datasets and high-dimensional feature spaces. The working mechanism of SVM is illustrated in Fig. 1b [40]. The core principle of SVM involves minimizing structural risk to reduce generalization errors by identifying the optimal separating hyperplane (OSH) between two classes of samples, thereby maximizing the inter-class margin. This is achieved through constructing optimal regression hyperplanes in high-dimensional feature spaces [41,42]. SVM has become one of the most widely used machine learning algorithms, extensively applied to pattern classification and regression problems. Notably, SVM can effectively address key challenges in high-dimensional data processing, including convergence difficulties, high computational complexity, and poor interpretability of results. This unique capability makes SVM particularly well-suited for intelligent identification of sparse bubble (non-overlapping) flow patterns in microchannels [43]. Consequently, in recent years, SVM has been increasingly employed by researchers to investigate flow pattern recognition and surface texture characterization in microchannel flows. However, SVM also has limitations including slow convergence and long training times. To address these issues, researchers have developed various improved algorithms that enhance training efficiency while maintaining acceptable accuracy levels [39]. For instance, Xie [44] introduced regularized multi-view least squares twin support vector machines, while Gendeel et al. [45] proposed a wind farm prediction method combining variational mode decomposition with the least squares support vector machine (LS-SVM) for deterministic and probabilistic interval forecasting.

2.1.2 Unsupervised Learning (UL)

UL is a machine learning paradigm that does not rely on labeled data, and achieves learning goals by independently exploring the internal structure and distribution of data. Unlike SL, UL does not require pre-defined output labels but automatically identifies latent data patterns through algorithms, making UL particularly suitable for scenarios with unknown sample categories. This method provides an effective tool for feature extraction and pattern recognition of complex systems by mining the statistical characteristics of the data itself.

UL algorithm system is abundant, mainly including clustering analysis and dimensionality reduction technology. In cluster analysis, the K-means clustering algorithm is the most widely used algorithm, which starts from k random clustering centers and then divides a set of objects into k subsets, which is one of most well known of the partitioning methods widely used in clustering [46]. Fig. 2a [47] presents the taxonomy of K-means algorithm variants. The K-means clustering algorithm can discover the hidden cluster structure in the dataset and has been widely used and extended in various fields [48,49], which can be effectively applied to flow classification in two-phase flow pattern identification, but K-means has two drawbacks: sensitivity

to the initial value and easy to be trapped in the local optimal value. Principal component analysis (PCA) is a basic mathematical tool in dimensionality reduction techniques [50]. PCA is used as a linear transformation method to map the raw data to a low-dimensional space, retaining the most important features and reducing the dimensionality of the data [51]. PCA simplifies the measurement process, reduces the dependence on user input, and shortens the measurement time [36], which can efficiently realize the feature extraction and visual analysis of high-dimensional data of boiling heat transfer, and provide important support for the study of complex heat transfer phenomena.

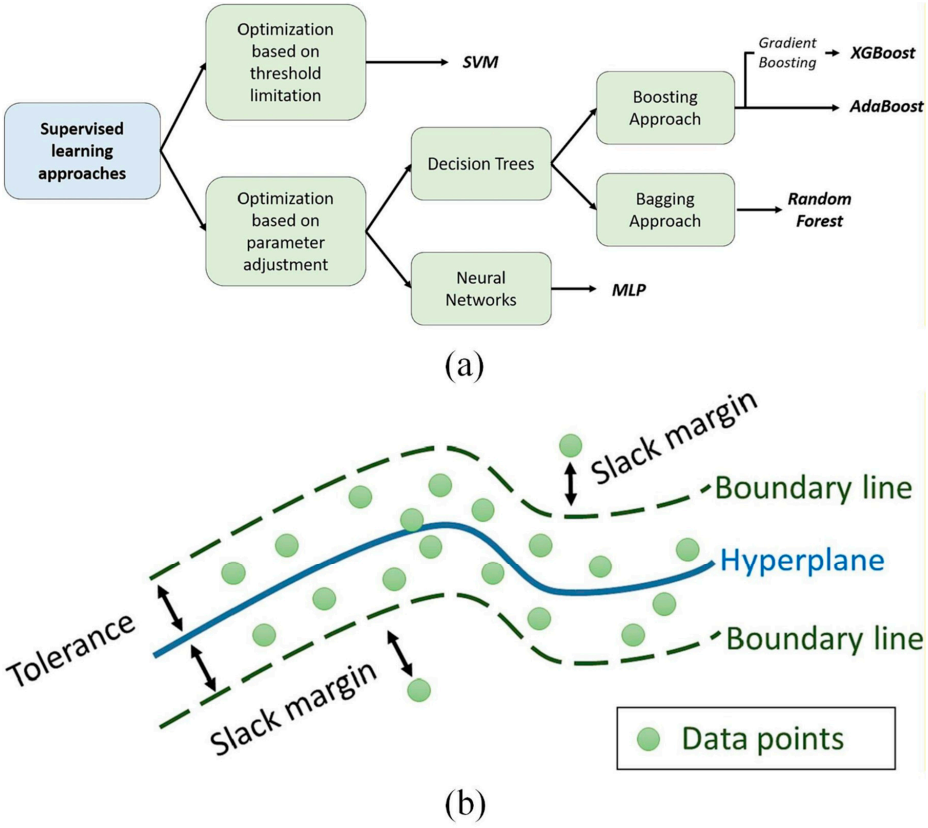

Figure 1: (**a**) Classification of SL. Reprinted from [38] (CC BY-NC-ND 4.0); (**b**) Schematic of the SVM methodology. Adapted from [40] (CC BY 4.0).

It is worth noting, however, that PCA is inherently limited to capturing linear relationships. Boiling image data often contains complex nonlinear structures arising from bubble interactions, deformations, and overlapping patterns. To address this, more advanced nonlinear dimensionality reduction techniques have emerged from the deep learning community. Autoencoders, particularly convolutional autoencoders, learn compressed latent representations through neural network architectures, enabling them to capture nonlinear features directly from raw bubble images. For visualization tasks, t-distributed stochastic neighbor embedding (t-SNE) and uniform manifold approximation and projection (UMAP) excel at preserving local neighborhood structures, making them particularly effective for revealing clusters of similar bubble regimes or flow patterns. While PCA remains valuable for its computational efficiency and interpretability, these nonlinear methods offer complementary strengths: autoencoders for feature learning in predictive modeling, and t-SNE/UMAP for exploratory visualization of complex boiling phenomena. The choice among these

techniques depends on whether the research priority is interpretability, nonlinear feature extraction, or high-quality visualization.

The K-means clustering algorithm effectively evaluates bubble nucleation sites, as demonstrated in Fig. 2b [52]. For intelligent identification of boiling heat transfer images, PCA can be integrated with bidirectional long short-term memory networks to form PCA-BiLSTMs, with performance results shown in Fig. 2c [53]. Both algorithms have been successfully applied, providing an effective solution for two-phase manifold identification and heat transfer feature extraction.

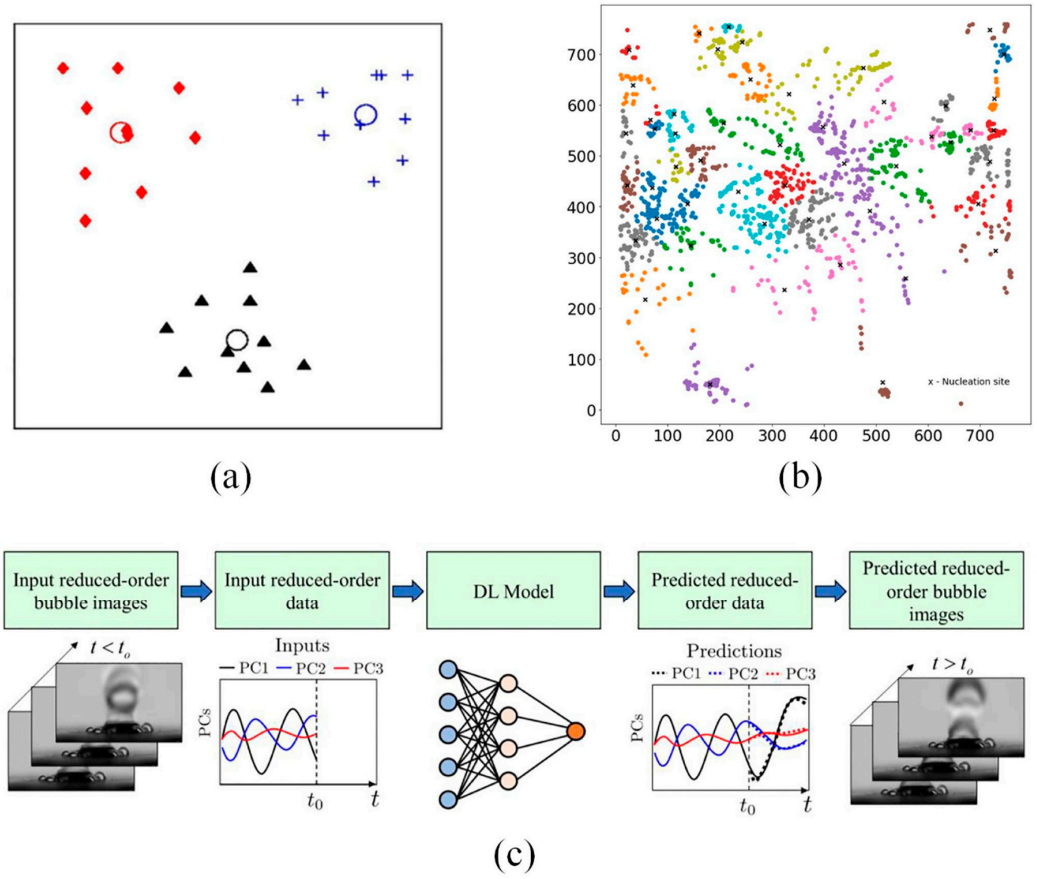

Figure 2: (**a**) Illustration of K-means algorithm. Adapted with permission from [47]. Copyright 2023, Elsevier; (**b**) K-means clustering algorithm to evaluate nucleation sites. Reprinted from [52] (CC BY 4.0); (**c**) Schematic diagram of the PCA-BiLSTM framework. Reprinted with permission from [53]. Copyright 2022, Elsevier.

2.1.3 Reinforcement Learning (RL)

RL is a machine learning paradigm based on the interaction between the agent and the environment, and the core of RL is to make the agent learn the optimal strategy step by step through a trial-and-error mechanism to achieve a specific goal or maximize the cumulative reward. RL uses a well-designed reward function to guide the agent to choose the optimal action strategy in a specific state, so as to maximize the long-term return. In a complex and uncertain environment, the agent can dynamically optimize the decision-making strategy through real-time analysis of environmental feedback, gradually converge to the global optimal solution, and finally maximize the system performance. Despite the rapid development of RL, challenges remain, especially in fluid mechanics, where RL is still difficult to obtain complex scenarios for specific reward functions [39].

RL also shows significant application potential in boiling heat transfer research, and is often used to guide stochastic algorithms for constrained optimization. Radaideh et al. [54] proposed an innovative physics-driven RL optimization framework for boiling water reactor (BWR) fuel assemblies. Their approach utilized industrial-grade simulation codes (CASMO4 for radial optimization and SIMULATE3 for axial optimization) to achieve co-optimization. As shown in Fig. 3, this framework successfully enabled large-scale optimization design of BWR fuel assemblies. The optimization model not only shows excellent performance, but also proves that the proposed neuroevolutionary method has excellent versatility and portability, and can be generalized to other nuclear reactor component design optimization tasks with only a few adjustments.

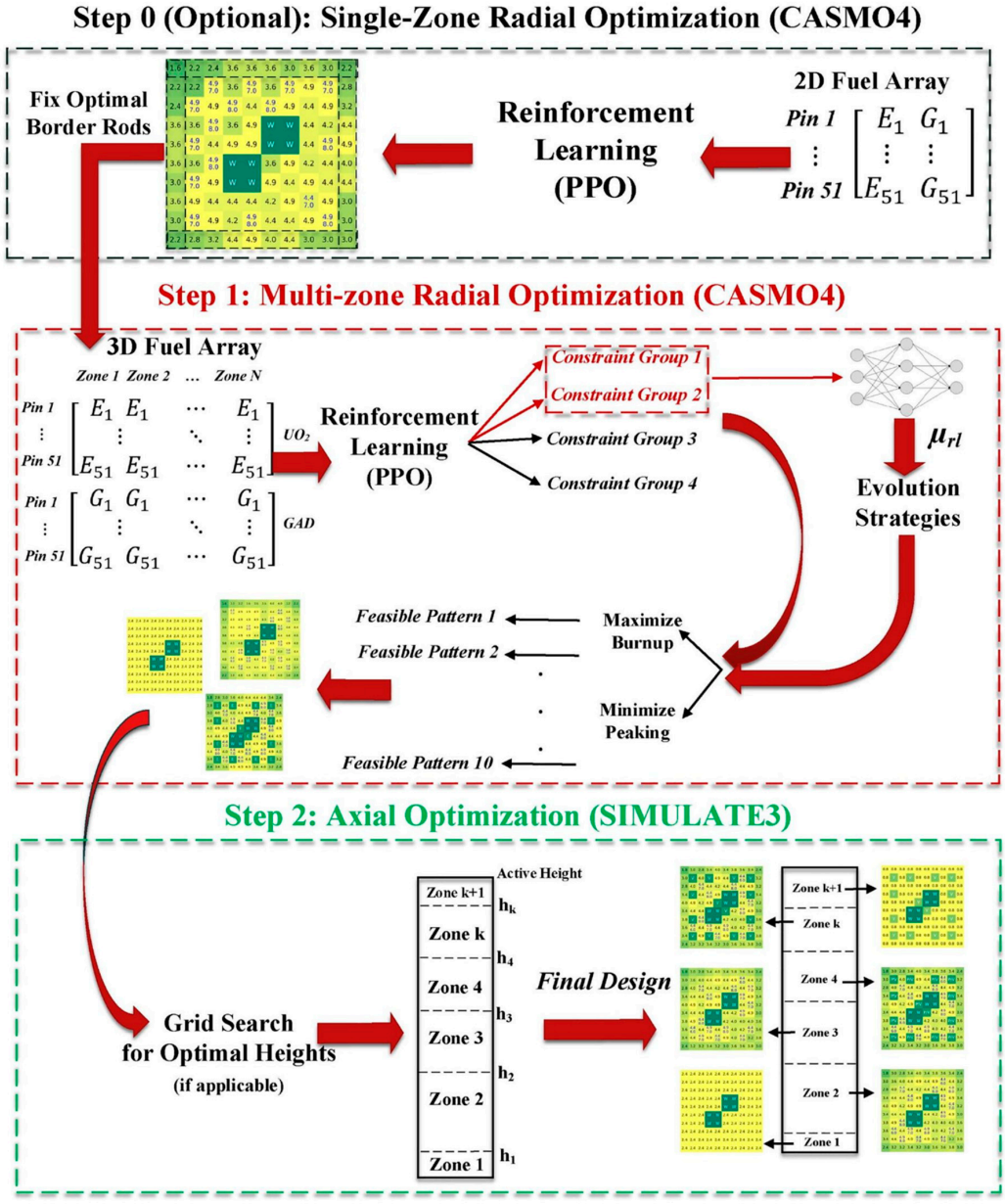

Figure 3: Flow diagram of the neuroevolutionary optimization bundle. Reprinted with permission from [54]. Copyright 2021, Elsevier.

2.2 Deep Learning (DL)

By building and training multi-layer neural network models, DL can automatically extract high-level features from massive data, so as to realize intelligent processing and decision-making of complex tasks. As an extension and development of artificial neural networks, DL has benefited from breakthroughs in big data technology and significant improvements in computing hardware performance in recent years, and has made breakthroughs in both theoretical research and practical application. The core of the project is to automatically learn the internal rules and feature representations of data through the deep network structure, which provides a powerful tool for the modeling and optimization of complex systems.

2.2.1 Multilayer Perceptron (MLP)

MLP is a typical feedforward neural network structure consisting of an input layer, at least one hidden layer, and an output layer, as schematically shown in Fig. 4 [55]. Each level contains multiple neural nodes, and the output is generated by weighted summing of input signals and processing by a nonlinear activation function. MLP can effectively solve classification and regression problems, and has shown a wide range of applicability in practical application scenarios such as image recognition, predictive analysis, and regression modeling. However, since each neuron in MLP is connected to every other neuron, fully connected networks often have many parameters, which makes them susceptible to overfitting when processing high-dimensional data [39].

In the field of boiling research, MLP, as the core tool of artificial intelligence modeling, has shown excellent application value in the study of key problems such as bubble dynamics analysis, boiling curve prediction and compound boiling point estimation, and provides strong technical support for the intelligent analysis of complex heat transfer processes.

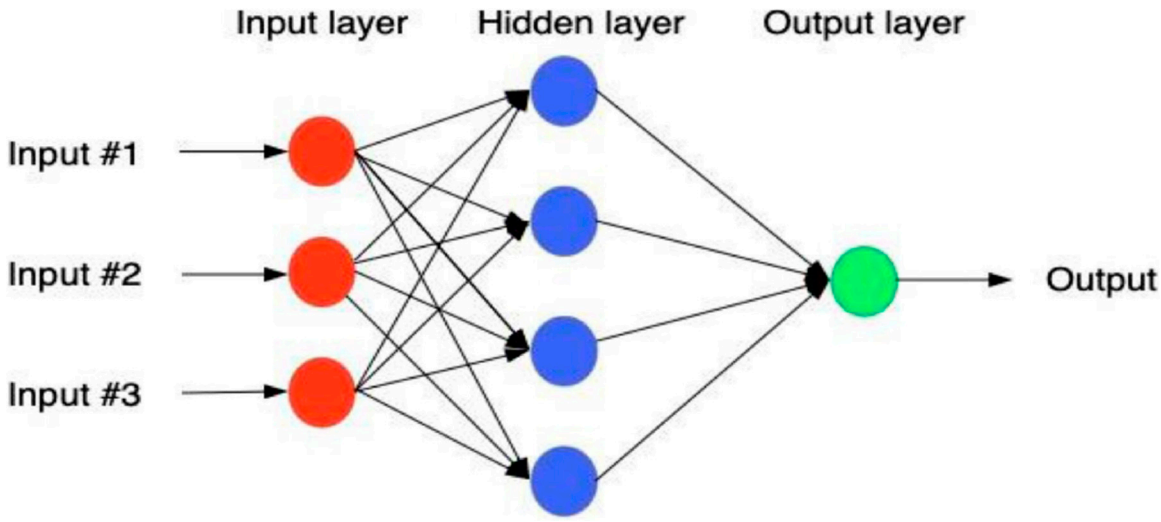

Figure 4: Schematic diagram of MLP structure. Reprinted with permission from [55]. Copyright 2022, Elsevier.

2.2.2 Convolutional Neural Network (CNN)

As one of the most representative algorithms in the field of DL, CNN is a feedforward neural network incorporating convolutional operations. The architecture of CNN is shown in Fig. 5 [56]. Despite increasing complexity and variability, these networks are essentially made up of basic elements [39], with typical structures including an input layer, a convolutional layer, an activation layer, a pooling layer, a fully

connected layer, and an output layer. The convolutional layer extracts spatial features through local receptive fields and weight sharing, introduces nonlinearity via activation functions, achieves feature dimensionality reduction and spatial invariance in the pooling layer, and finally performs feature integration and classification through the fully connected layer. This unique structure makes CNNs perform well in computer vision tasks such as image segmentation and object detection, and promotes the breakthrough development of visual perception technology.

In the study of boiling heat transfer, CNNs have shown unique application value in the field of bubble dynamics analysis with its powerful image processing capabilities. The researchers mainly focus on three key directions: intelligent identification of bubble characteristics, accurate segmentation of overlapping bubbles, and efficient reconstruction of occluded bubbles, which provides a new technical means for the quantitative analysis of boiling heat transfer phenomena.

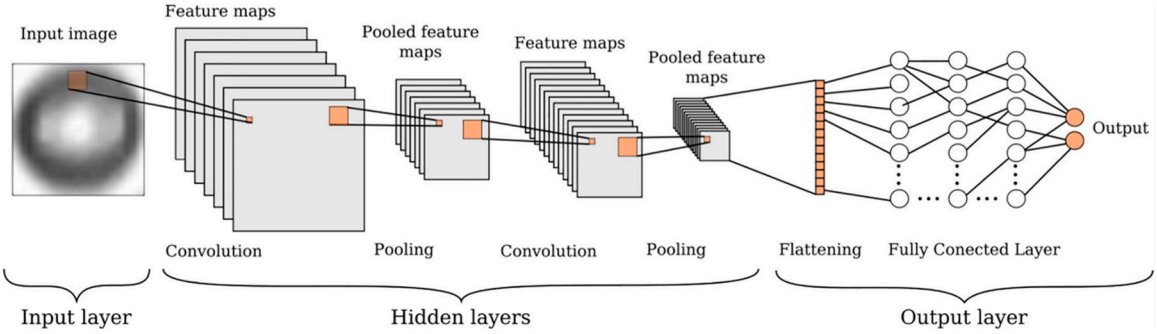

Figure 5: Example of CNN architecture. Reprinted with permission from [56]. Copyright 2021, Elsevier.

2.2.3 Recurrent Neural Network (RNN)

RNNs are neural network architectures specifically designed for sequential data processing. Their unique cyclic connections enable effective capture and modeling of temporal dependencies. RNNs demonstrate superior performance in areas such as natural language processing, time series analysis, speech recognition, and music generation, providing a powerful tool for solving complex problems with temporal characteristics.

Long short-term memory networks (LSTMs), as important variants of RNNs, have shown significant application potential in boiling heat transfer research. LSTMs employ memory cells and three nonlinear gates to replace RNN's basic activation units. This architecture enables selective forgetting of irrelevant historical information while evaluating current inputs and retaining useful features in memory cells [57,58]. Compared to traditional RNNs, LSTMs demonstrate superior capability in learning long-term temporal dependencies. However, the original LSTM formulation fails to consider correlations between predicted quality variables and input samples [59]. LSTMs are frequently integrated with complementary algorithms for boiling heat transfer applications. As illustrated in Fig. 6, architectures like the Spatiotemporal Attention-based LSTM (STA-LSTM) enable both parameter prediction and boiling regime identification.

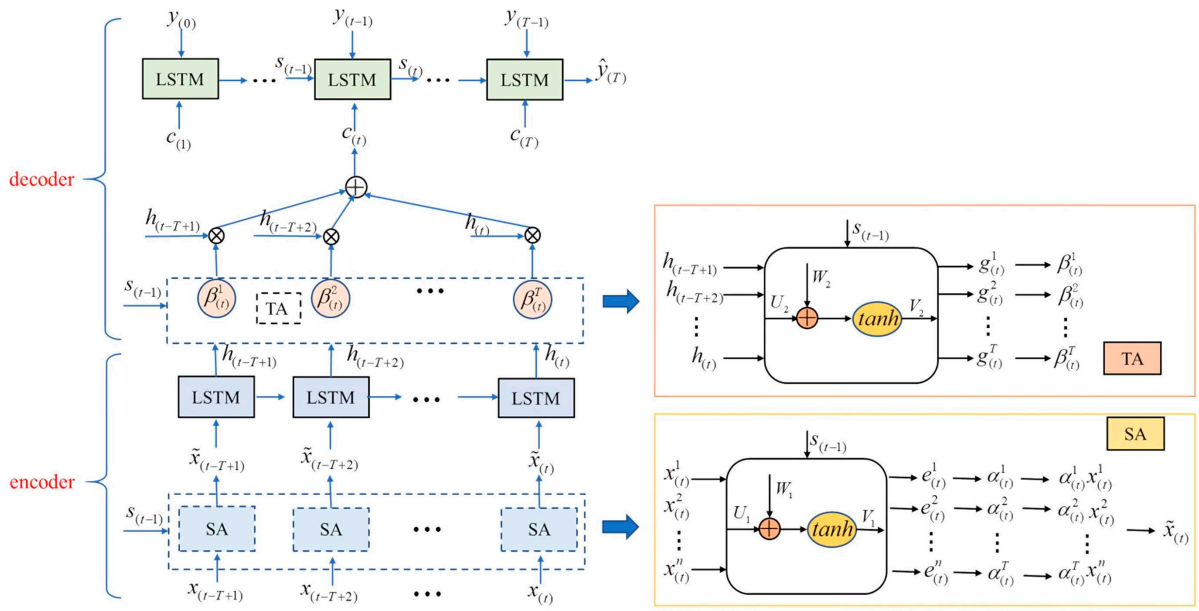

Figure 6: Spatiotemporal attention-based LSTM framework. Reprinted with permission from [59]. Copyright 2021, IEEE.

2.2.4 Attention Mechanism and Transformer

The attention mechanism has emerged as a powerful technique that enables neural networks to dynamically focus on the most relevant parts of the input when generating outputs. Unlike recurrent architectures that process data sequentially, attention computes a weighted sum of all input elements, where the weights reflect the importance of each element for the current task. This allows the model to capture long-range dependencies more effectively and supports parallel computation, overcoming key limitations of RNNs.

The Transformer model, a breakthrough in neural network architecture, has significantly advanced the field of machine learning, particularly in natural language processing. Central to its success is the self-attention mechanism, which dynamically assigns importance to different parts of the input, greatly enhancing the model's ability to discern context and relationships within the data. This feature is not only advantageous in processing sequential data but also proves beneficial in understanding spatial relationships, making it applicable to a variety of data types, including point data [60]. A Transformer typically consists of an encoder and a decoder. The encoder reads the input data and the decoder produces the prediction. Within these components, multiple layers of self-attention and feed-forward networks interact to refine the data representation.

In boiling heat transfer research, Transformer-based models have demonstrated exceptional performance in predicting Critical Heat Flux (CHF), as detailed in Section 3.1.1. Their ability to model complex nonlinear relationships among multiple input parameters makes them particularly suitable for such predictive tasks, often outperforming traditional machine learning approaches. This success underscores the growing potential of attention-based architectures for advancing thermal-fluid sciences.

3 Prediction in Boiling Heat Transfer Characteristic

Predicting boiling heat transfer characteristics—CHF, HTC, and boiling curves—has long been a central challenge in the field. The studies reviewed in this section represent some of the earliest and most extensive

applications of AI to boiling problems, establishing foundational capabilities that later innovations would build upon. Early efforts focused on demonstrating that machine learning models could match or exceed traditional correlations, while more recent work has begun to introduce architectural innovations—such as Transformers and hybrid frameworks—that address the limitations of these initial approaches.

3.1 Boiling Heat Transfer Parameter

The accurate prediction of boiling heat transfer characteristic parameters represents a critical aspect of boiling heat transfer research, with Critical Heat Flux (CHF), Heat Transfer Coefficient (HTC) and Onset of Nucleate Boiling (ONB) being the three most pivotal parameters. As the critical boundary of heat transfer mode, CHF is an important threshold for heat transfer engineering design and safety assessment [60]. HTC is the core parameter for characterizing boiling performance, which is related to the bubble dynamics near the boiling surface [61]. ONB signifies the beginning of vapor bubble formation and represents the transition from the initial single convective region to the coexistence of liquid and gas phases [62]. These parameters serve not only as fundamental data for constructing boiling curves but also as critical design criteria in engineering practice. In recent years, the rapid advancement of AI technology has motivated numerous researchers to explore AI-based prediction methods for CHF and HTC, thereby providing innovative technical approaches for boiling heat transfer research. However, due to the relatively limited research on AI models for predicting ONB, this section will not provide a detailed discussion on this aspect. Instead, we will systematically review the application of AI technologies in CHF and HTC prediction, and examine their innovative advancements in boiling curve prediction.

3.1.1 CHF

The prediction of CHF mainly relies on two methods: one is to develop empirical correlation based on experimental data, and the other is to use the surrogate model to construct a prediction model. However, when these methods are extended beyond their original parameters, significant uncertainty often arises, limiting their scope of application [60].

In recent years, researchers have been actively exploring the application of artificial intelligence technology in CHF prediction to improve the prediction accuracy and generalization ability. Cabarcos et al. [38] and Kumar et al. [63] explored the performance of traditional AI models such as SVM and ANN in predicting CHF. Cabarcos et al. [38] conducted a systematic comparison of five SL algorithms (ANN, SVM, AdaBoost, RF, and XGBoost) for CHF prediction using 5-fold cross-validation across three task modules. In the classification-oriented first two modules, SVM demonstrated superior robustness, achieving test precision of 0.876 and recall consistently above 0.8. In the regression-based third module, SVM again performed well with normalized mean absolute error (nMAE) ranging from 5.58% to 6.56% and a test R^2 of 0.891. The ANN model, as illustrated in Fig. 7a, exhibited comparable regression errors (nMAE ~6%, nRMSE ~8%) but showed signs of overfitting, with its coefficient of determination dropping from 0.933 during training to 0.844 during validation. These findings validate the effectiveness of ML techniques for boiling prediction while highlighting the importance of assessing generalization. Kumar et al. [63] compared RF, SVM, and ANN for CHF location prediction against experimental data from Becker et al. [64]. As shown in Fig. 7b, the ANN model achieved outstanding performance, with test mean absolute percentage error (MAPE) of 6.04%, test R^2 of 0.9404, and all test points falling within an absolute relative error of 0.25, confirming its superior predictive capability and reliability.

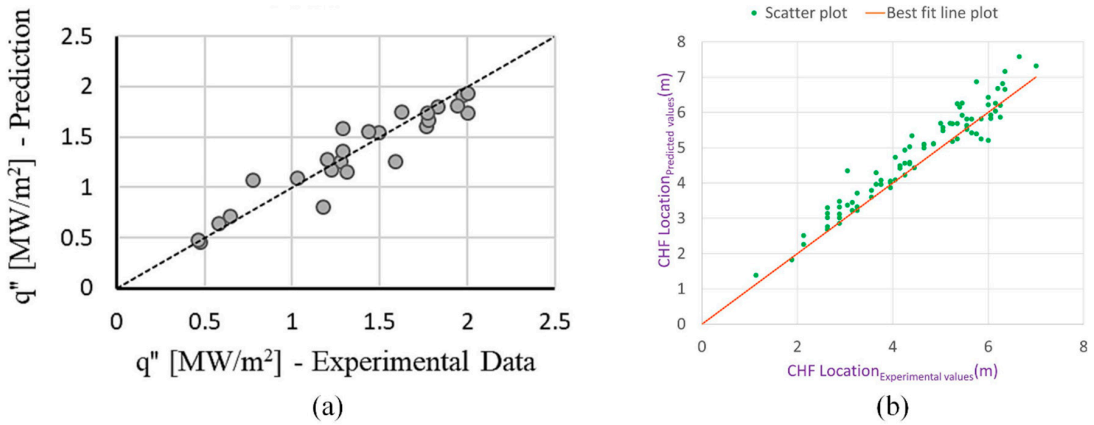

Figure 7: (**a**) ANN test results of Cabarcos et al. Reprinted from [38] (CC BY-NC-ND 4.0); (**b**) ANN test results of Kumar et al. Reprinted with permission from [63]. Copyright 2024, Elsevier.

Among these, the Transformer architecture—introduced in Section 2.2.4—has garnered particular attention due to its superior performance in handling complex, multi-dimensional input data. Zhou et al. [60] and Wang et al. [65] found that the Transformer model also performed well in CHF prediction. Zhou et al. [60] systematically optimized the architectures of ANN, CNN, and Transformer models, comparing their predictive performance through the Optuna framework. As illustrated in Fig. 8a, results demonstrated that the five-input Transformer model achieved optimal performance, with a mean prediction-to-measurement ratio of 1.008 (indicating a slight average overprediction of just 0.8%), a MAPE of 7.22%, and a RMSPE of 12.3% [60]. This model was subsequently employed as a pre-trained model for transfer learning, significantly reducing prediction errors. Wang et al. [65] conducted a comparative analysis of CHF prediction performance among Transformer, Mamba, and Temporal Convolutional Network (TCN) models. The results are presented in Fig. 8b. Their findings revealed that the Transformer approach outperformed conventional models including Random Forest, Bayesian Linear Regression, and Backpropagation Neural Network (BPNN) in terms of both predictive accuracy and stability, achieving a MAPE of 4.57%, RMSPE of 9.85%, and a Q^2 value of 0.57%, indicating superior predictive accuracy and stability [65].

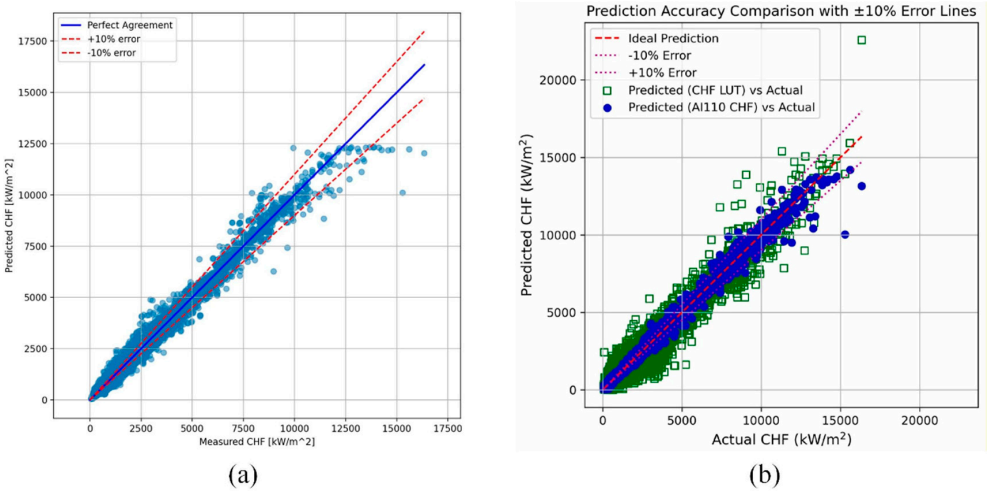

Figure 8: (**a**) Zhou et al., five input Transformer model prediction results. Reprinted from [60] (CC BY-NC 4.0); (**b**) Wang et al. model prediction results. Adapted from [65] (CC BY-NC 4.0).

Building upon these foundations, Khalid et al. [66] proposed a hybrid model integrating Deep Sparse Autoencoder (AE) and Deep Neural Network (DNN) to enhance model generalizability. By utilizing concatenated features extracted by AE as input for CHF prediction, their experimental results demonstrated superior accuracy, significantly outperforming conventional ML models including LUT, SVM, and ANN. The results are presented in Fig. 9a. To further enhance model interpretability, Sajjad et al. [67] employed DNNs with SHAP-based explainable AI (XAI) and sensitivity analysis, achieving an overall R^2 of 0.97. Their analysis identified surface inclination as the most influential parameter, with its exclusion causing a 30% deviation in predicted CHF values, followed by liquid saturation temperature (22% deviation), material thermal conductivity, surface roughness (18% deviation), and finally operational pressure as the least sensitive parameter (0.16% deviation) [67]. This dual focus on accuracy and interpretability demonstrates how AI can not only predict but also reveal underlying physical sensitivities in boiling crisis phenomena.

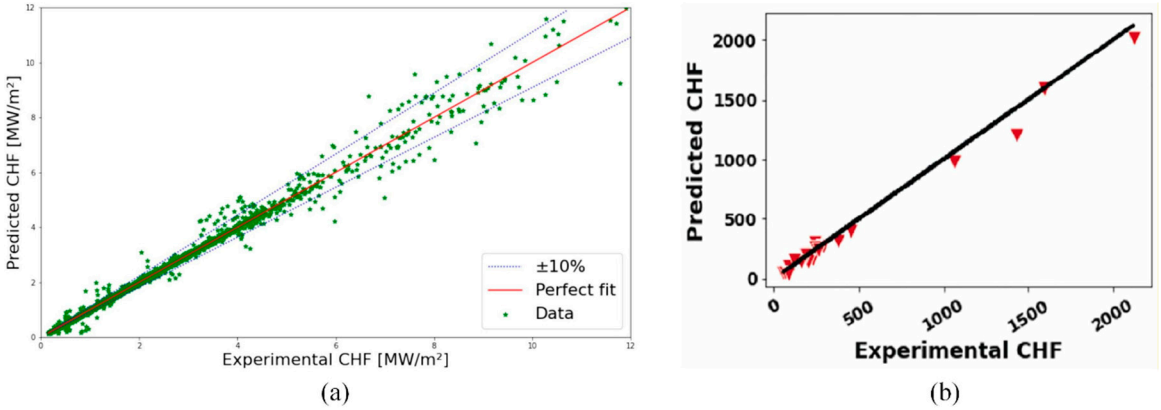

Figure 9: (**a**) Prediction results of Khalid et al.'s model. Reprinted with permission from [66]. Copyright 2024, Elsevier; (**b**) Prediction results of Sajjad et al.'s model. Reprinted from [67] (CC BY-NC-ND 4.0).

The evolution of AI tools for CHF prediction demonstrates a clear technological trajectory: Foundational models including SVMs and ANNs [38,63] establish efficiency benchmarks in resource-constrained environments, while performance-enhanced architectures like Transformers [60,65] achieve unprecedented accuracy under complex conditions at the cost of significant computational resources. This paradigm is now advancing toward innovative fusion frameworks such as DNN-AE and DNN-XAI hybrids [66,67], which balance interpretability with generalization capabilities across diverse operational scenarios. The progression from efficiency-focused foundations, through precision-oriented enhancement, toward converged balance defines the next frontier in boiling heat transfer modeling. It is worth noting, however, that this pursuit of accuracy often comes at the expense of interpretability. Transformers and other deep learning architectures, despite their predictive power, function largely as "black boxes" that offer limited direct physical insight into the boiling crisis mechanisms they model [34,35]. This trade-off between precision and explainability has motivated the emergence of fusion frameworks such as DNN-AE and DNN-XAI hybrids [66,67], which explicitly aim to balance predictive performance with interpretability. This progression from foundational models to fusion frameworks is quantitatively evidenced in key performance metrics as shown in Table 1. A cross-analysis of the models presented in Table 1 reveals a consistent trend of high predictive accuracy, with reported performance metrics typically reaching R^2 values above 0.89. The consistently high accuracy of these AI models, as summarized in Table 1, marks a substantial improvement over classical correlations such as Zuber [5], which are inherently limited by their simplifying assumptions

and typically exhibit substantially larger errors and poorer generalization compared to the data-driven AI models reviewed herein.

Table 1: Evolutionary progression of AI models in CHF prediction performance.

Model Type	Example	Key Performance
Foundational Models	SVM, ANN [38,63]	$R^2 > 0.89$
Enhanced Architectures	Transformer [60,65]	MAPE < 7.5%
Fusion Frameworks	DNN-AE, DNN-XAI [66,67]	$R^2 = 0.97$

3.1.2 HTC

For decades, researchers have developed empirical models for HTC prediction, yet these models exhibit significant deviations (±40~50% error margins [68,69]) when applied to different surface geometries or operational conditions. To overcome these limitations of conventional approaches, current research focuses on developing AI-based high-precision HTC prediction models, aiming to enhance both adaptability across varying working conditions and predictive accuracy.

Sajjad et al. [70] and Ayoobi et al. [71] have focused on developing higher-accuracy AI models to investigate the impact of individual variables (refrigerant type, water hardness) on boiling heat transfer performance. Sajjad et al. [70] pioneered a hybrid model integrating DNN and Genetic Algorithm (GA) for predicting and optimizing flow boiling heat transfer coefficient (FBHTC) in micro/mini-channels. Across multiple refrigerants, the model demonstrated exceptional accuracy, achieving an R^2 of 0.988 and a mean squared error (MSE) of just 0.05% [70], with results showing excellent agreement with experimental data in Fig. 10a. This fully validates robustness and reliability of the hybrid model. Ayoobi et al. [71] investigated the effect of water hardness on transient pool boiling by employing ANN to predict HTC across varying time intervals and hardness levels. The study compared experimentally obtained HTC and heat flux values with network predictions. As demonstrated in Fig. 10b, results showed excellent agreement between the test network's predictions and experimental values. The network achieved a test R^2 of 0.981 with a mean absolute error (MAE) of 1.535%, indicating high predictive accuracy that could substantially reduce experimental and time costs [71]. Although localized discrepancies in HTC point distributions were observed in some cases, the overall predictions exhibited statistically significant correlation with actual measurements, conclusively validating the ANN model's reliability and accuracy in heat transfer coefficient prediction.

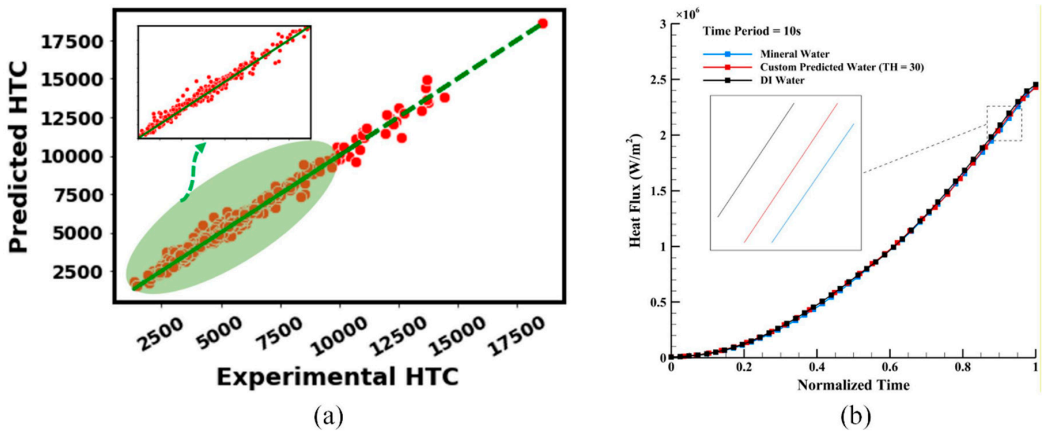

Figure 10: (**a**) HTC prediction data from the DNN model. Reprinted with permission from [70]. Copyright 2024, Elsevier; (**b**) Heat flux prediction from the ANN model. Reprinted with permission from [71]. Copyright 2024, Elsevier.

Building upon single-variable investigations of boiling heat transfer performance, Mehdi et al. developed higher-accuracy predictive models specifically for enhanced surface boiling characteristics [61,72]. To accurately predict pool boiling heat transfer on various enhanced surfaces, Mehdi et al. [72] investigated complex relationships among four geometric parameters, nine thermophysical properties, and two operational conditions, developing a DNN-based model for enhanced-surface HTC prediction. The comparative analysis with existing empirical models revealed that this model reduces MAPE in pool boiling HTC prediction by at least 20% [72]. When validated against existing experimental datasets not included in the training process, the pre-trained model predicted 84% of data points within ±30% error bounds (20% MAPE), substantially outperforming conventional empirical correlations, which typically achieve only 40% within the same bounds (38% MAPE) [72], as illustrated in Fig. 11a To accurately predict enhanced heat transfer performance on microstructured surfaces, Mehdi et al. [61] employed three deterministic ML models (RF, DNN, and 1D-CNN) and two probabilistic models (NG Boost and BNN) for HTC prediction on enhanced surfaces. They introduced dimensionless numbers as input-output parameters, utilizing deterministic models to predict the Nusselt number (Nu) while employing probabilistic models for optimization. Experimental results demonstrated that the optimized models exhibited superior predictive performance on test datasets, showing excellent agreement between experimental and predicted values. All artificial neural network models achieved MAPE less than about 15% on test data, as illustrated in Fig. 11b. Further analysis using SHAP identified the boiling Reynolds number, kinetic Reynolds number, and Boiling number as the most critical parameters; excluding the least influential parameters increased MAPE only marginally—from 4.58% to 4.72% for the DNN and from 13.4% to 16.14% for RF—validating the robustness of the key parameter identification [61].

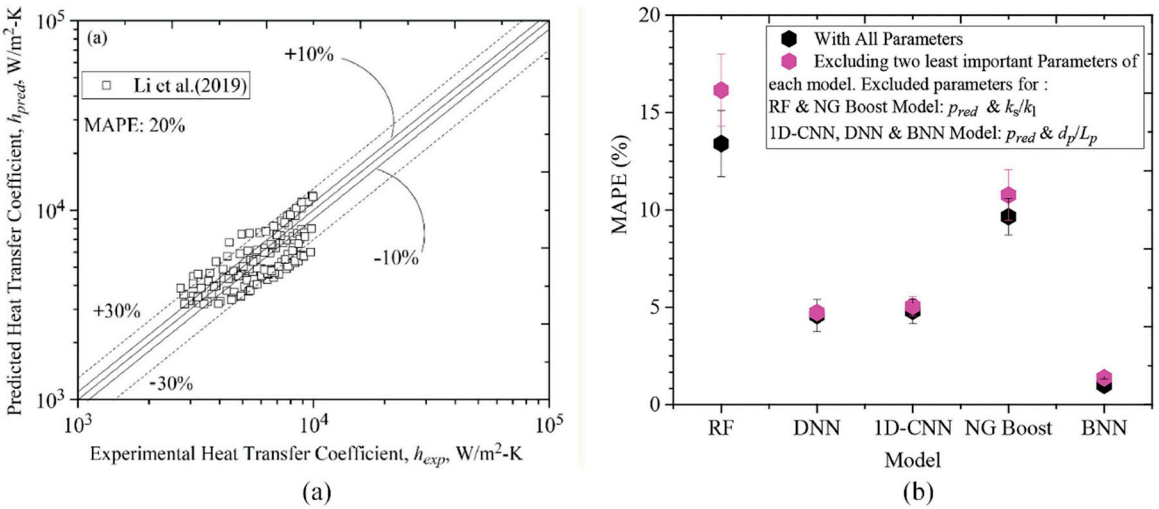

Figure 11: (**a**) HTC prediction data from the DNN model. Adapted with permission from [72]. Copyright 2022, Elsevier; (**b**) Mean absolute percentage error (MAPE) of all models. Reprinted from [61] (CC BY-NC 4.0).

Building upon advancements in enhanced surface prediction accuracy, Sajjad et al. further developed generalized AI models to predict boiling heat transfer performance across diverse complex surface conditions, including the effects of varying coating characteristics and surface roughness [73,74]. To accurately predict pool boiling performance on various coated nanoporous surfaces, Sajjad et al. [73] developed a DL technique for HTC prediction and extended applicability of the prediction across a broad parameter range. Through systematic data collection, feature engineering, and optimization of hidden layer architectures,

they identified an optimal configuration achieving an R^2 of 0.9988, average absolute relative deviation (AARD) of 3.272%, and mean absolute error (MAE) of 1.77% [73]. As demonstrated in Fig. 12a, these models outperform existing empirical approaches in both prediction accuracy and operational simplicity. The DL approach exhibits wide applicability, generalizable to diverse working fluids and experimental conditions. Building upon this breakthrough, Sajjad et al. [74] proposed a universal DL approach for predicting nucleate boiling performance across surfaces with varying roughness. Through systematic training of different DNN architectures, they identified an optimal configuration achieving an overall R^2 of 0.994, AARD of 13.7%, and MAE of 0.65 for the predicted boiling heat transfer coefficient (BHTC) [74]. This methodology accurately predicts the boiling heat transfer coefficient (BHTC) for diverse solid-liquid combinations, applicable to multiple working fluids (including water, dielectric liquids, and refrigerants) and surface treatments (such as polished, machined, and sandblasted surfaces). Experimental validation results are presented in Fig. 12b, demonstrating the model's comprehensive parameter coverage and exceptional accuracy in BHTC prediction. The DL model's boiling heat transfer coefficient prediction in Fig. 12 demonstrates unprecedented generalization across surface treatments and working fluids.

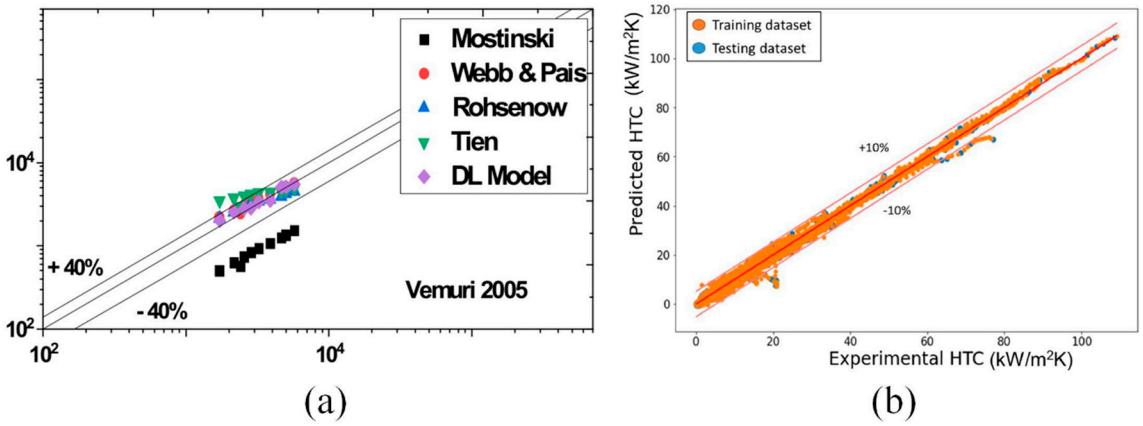

Figure 12: (**a**) Comparison of HTC predictions between DL models and existing models. Adapted from [73] (CC BY 4.0); (**b**) BHTC prediction performance of the DL model. Reprinted with permission from [74]. Copyright 2021, Elsevier.

The evolution of HTC prediction tools can be summarized in three key phases. Firstly, ANNs applied to single-variable analyses proved effective for parameter-specific problems, yielding R^2 over 0.98 in controlled settings. This high predictive accuracy effectively validated the approach. Secondly, the focus shifted to precision, with DNNs that fuse multiple geometric-thermophysical features to reduce MAPE below 15% by modeling complex, non-linear interactions. Finally, the field has advanced towards generalization, where deep learning models maintain high accuracy across different conditions, significantly outperforming empirical correlations. The progression outlined in Table 2 is quantitatively grounded. As the table demonstrates, advanced models consistently achieve a high level of accuracy, with R^2 frequently exceeding 0.98 [70,71,73,74], while also reducing predictive errors such as MAPE to below 20% [61,72], a substantial improvement over classical correlations. For instance, the developed DL models maintain $R^2 > 0.99$, effectively eliminating the large deviations that plague classical HTC correlations such as Rohsenow, Cooper, Gorenflo, and Leiner correlations [73,74] on non-ideal or enhanced surfaces. The performance metrics reported in each source study are heterogeneous; therefore, our table employs the respective metrics used in the original publications.

Table 2: Performance Evolution of HTC Prediction Models.

Development Stage	Model Type	Accuracy
Parameter-Specific Analysis	DNN, ANN [70,71]	$R^2 > 0.98$
Geometric-Thermophysical Fusion	DNN Hybrid [61,72]	MAPE < 20%
Industrial Generalization	DL [73,74]	$R^2 > 0.99$

It is worth noting that despite the high predictive accuracy reported in the studies reviewed above, a fundamental challenge persists: experimental boiling data for nominally identical surfaces often exhibit significant variations across different laboratories due to differences in apparatus, ambient conditions, and measurement protocols. When such heterogeneous multi-source data are used for training, conventional performance metrics (e.g., R^2, MAPE) may not fully capture a model's true generalizability. Addressing this requires evaluation strategies that extend beyond single-dataset hold-out tests, such as cross-dataset validation and uncertainty quantification, to ensure model robustness across diverse experimental conditions [61]. Looking forward, transfer learning and domain adaptation techniques offer promising pathways toward developing AI models that can generalize across laboratory-specific biases with minimal retraining [60]. The studies reviewed above reveal a consistent pattern: architectures capable of capturing long-range dependencies and complex feature interactions—particularly Transformers and hybrid DNN models—consistently outperform traditional machine learning methods in CHF and HTC prediction tasks [60,65,66]. This is not coincidental. Boiling heat transfer parameters are governed by multiple, interacting physical factors (surface properties, fluid characteristics, operating conditions) whose relationships are inherently nonlinear and non-local. Transformers, with their self-attention mechanisms, excel at modeling such multidimensional interactions without the sequential processing constraints of RNNs or the local receptive field limitations of CNNs. In contrast, while CNNs remain the dominant choice for image-based tasks, their application to scalar parameter prediction is less straightforward, requiring careful feature engineering or hybrid architectures [61]. What these successful models are implicitly learning, therefore, is a high-dimensional representation of the underlying physics—mapping input parameters to output quantities in a way that respects the governing thermodynamic principles, even if those principles are not explicitly encoded.

However, a note of caution is warranted regarding the exceptionally high R^2 values (>0.98 or >0.99) reported for many of these models. First, dataset size matters: many studies rely on relatively small datasets (hundreds to a few thousand data points) from single laboratories under controlled conditions [38,63]. High R^2 values can mask overfitting—the model may memorize dataset-specific noise rather than learning generalizable physics. This risk is particularly acute for complex architectures like Transformers, which require correspondingly larger datasets to avoid spurious correlations [60]. Second, cross-laboratory validation is essential but rarely performed; models that excel on one experimental facility often degrade on another due to differences in apparatus and protocols—a domain shift problem. Third, uncertainty quantification (UQ) should accompany point predictions, especially for safety-critical applications. Probabilistic models (e.g., Bayesian neural networks, Monte Carlo dropout) can provide prediction intervals that reflect both aleatoric and epistemic uncertainty [61]. Without such UQ, even models with $R^2 > 0.99$ may prove unreliable outside their training distribution. Future work should therefore move beyond point metrics toward holistic evaluation encompassing dataset transparency, cross-validation rigor, and uncertainty awareness.

3.2 Boiling Curve

CHF and HTC represent critical parameters of boiling curves, which serve as fundamental characterizations of liquid boiling heat transfer mechanisms. Traditional empirical correlations remain limited to specific parameter ranges, leaving the precise Q-ΔT relationship of boiling curves still dependent on experimental measurements. While existing models can predict heat flux within constrained temperature ranges, their generalization capabilities are severely limited [75]. To overcome these constraints, researchers have begun developing AI-based boiling curve prediction models with enhanced accuracy and generalization capacity, aiming to transcend the limitations of conventional approaches.

Scariot et al. [76] pioneered a CNN-based heat flux inference model utilizing visualization data, achieving precise boiling heat flux measurements without requiring bubble statistics, or hydrodynamic parameters, or expensive high-speed cameras. The model generated transient boiling curves as shown in Fig. 13a. Suh et al. [77] developed a data-driven learning framework correlating dynamic bubble imaging with boiling curves. They developed a Hybrid Physics-enhanced (HyPR) model by coupling CNN and MLP architectures. As shown in Fig. 13b, the HyPR model achieved a MAPE of 6%, outperforming the standalone CNN (MAPE = 15%) and MLP (MAPE = 8%) models. This demonstrates its superior predictive accuracy and minimal test loss in boiling curve prediction. Sajjad [75] established a DNN framework grounded in physical mechanisms and relevant features for pool boiling curve prediction. As demonstrated in Fig. 13c, this framework successfully predicts high-order boiling curves through integration of classical correlation models and physics-based inputs, while maintaining strong generalization across diverse solid-liquid combinations.

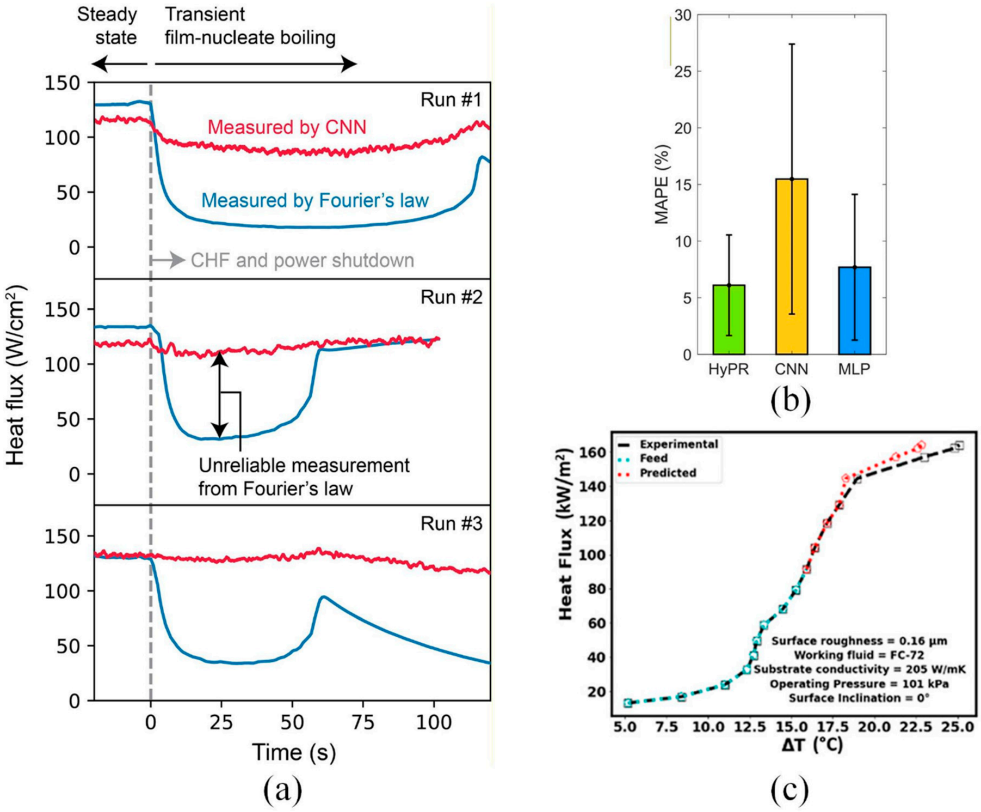

Figure 13: (**a**) Transient boiling curves from Scariot et al.'s model. Reprinted with permission from [76]. Copyright 2024, Elsevier; (**b**) Comparative analysis of Suh et al.'s model. Adapted from [77] (CC BY 4.0); (**c**) Boiling curve prediction using Sajjad's DNN framework. Adapted with permission from [75]. Copyright 2024, Elsevier.

The intelligent prediction of boiling curves has evolved through three distinct yet complementary approaches: Visualization-driven CNN models eliminate the need for bubble statistics but face limitations in generalizing to transient curve capture if the training dataset lacks coverage of diverse boiling regimes [76]; Hybrid Physics-enhanced (HyPR) frameworks dynamically correlate bubble dynamics with thermal responses, achieving optimal accuracy-efficiency trade-offs; and Physics-anchored DNNs integrate classical correlations to deliver high-order predictions with enhanced generalization. Collectively, these approaches demonstrate significantly lower prediction errors than conventional empirical correlations while maintaining robust cross-scenario stability, establishing a versatile toolbox for next-generation thermal system design.

4 Bubble Recognition and Detection of Dynamic Parameters

Currently, researchers are actively exploring AI technologies to achieve precise prediction and intelligent recognition of bubble dynamics, providing novel technical approaches for boiling heat transfer research. This section will comprehensively review advancements in AI applications for bubble image recognition and dynamic parameter prediction, encompassing core research directions such as bubble feature extraction, behavior analysis, and heat transfer performance prediction.

Bubble dynamics analysis presents a different class of problems—image segmentation, object detection, parameter extraction—that require spatially-aware architectures. The field again progressed from foundational models (U-Net, Mask R-CNN) that established what was possible, through refinements that addressed domain-specific challenges like overlapping bubbles, toward emerging frameworks that explicitly model bubble-bubble interactions.

4.1 Bubble Identification

Due to the inherent complexity and stochastic nature of bubble dynamics, compounded by extensive bubble-bubble interactions, conventional identification methods often face dual challenges of high costs and significant misjudgment rates. To address these limitations, AI technologies have been employed to enhance the accuracy of bubble recognition and analysis.

4.1.1 CNN-Based Methods

CNN models, with their powerful spatial feature extraction capabilities, form the backbone of modern bubble image analysis. These architectures are tailored to solve distinct types of tasks, primarily categorized into semantic segmentation and instance segmentation. The following subsections review these architectures based on their primary problem-solving paradigm.

Among various CNN variants, U-net and Mask R-CNN have garnered significant research attention due to their distinctive advantages. The core strength of U-net lies in its multi-level architecture combining upsampling and downsampling layers. This design enables the network to comprehensively incorporate global contextual image information while maintaining efficient training capability even with small-scale datasets [78]. U-net achieves classification errors below 2% through threshold adjustment and stochastic gradient descent optimization, leveraging exceptional cross-scale recognition capability of U-net [79]. Meanwhile, Mask R-CNN demonstrates superior performance in processing overlapping bubbles and complex flow patterns via its instance segmentation technology, which generates precise binary masks, bounding boxes, and class labels for each object in images [80]. The architecture's unique triple-output structure (masks, bounding boxes, and class labels) enables outstanding object recognition in complex

scenarios [81]. These CNN variants provide diversified technical options for boiling heat transfer research, significantly advancing the intelligent development of bubble dynamics analysis.

Semantic Segmentation with U-Net and Variants

U-Net has emerged as the predominant method for semantic segmentation of boiling heat transfer images, a task focused on pixel-wise classification. Its unique encoder-decoder architecture delivers exceptional performance in precisely delineating bubble regions. Ravichandran et al. [78] employed high-resolution optical phase detection data to train a U-net model for dryout region identification. They developed a U-net-inspired 3D CNN architecture, incorporating Adam optimizer and transfer learning for model optimization. Qualitative comparisons in Fig. 14a demonstrate U-net's precise dryout pattern segmentation when benchmarked against phase detection results. Across three representative cases, the model achieved optimal performance with accurate dryout region delineation. Furthermore, real-time dryout prediction experiments revealed that the U-net-based machine learning algorithm not only detects dryout regions with high precision but also enables quasi-real-time prediction [79], significantly enhancing the efficiency of dryout characterization; Schepperle et al. [82] utilized a customized U-net-based CNN to extract key features from video frames, incorporating real-time thermal imaging (RTD) technology to capture microchannel two-phase boiling videos and sensor data. Following preprocessing and binary image segmentation, they developed a DL model for flow regime classification and RTD data prediction. Results were shown in Fig. 14b. Experimental results demonstrated that the U-net-based CNN architecture achieved exceptional accuracy in both flow regime identification and void fraction prediction for microchannel flow boiling. Although the model exhibited suboptimal performance under certain flow velocity conditions, along with overfitting and limited generalization issues in RTD data, the trained DL model still delivered reliable predictive outcomes. While U-net establishes the state-of-the-art in bubble pattern extraction, its segmentation accuracy under extreme flow conditions can be compromised by image distortions. Enhancing the model's robustness to such turbulence-induced effects remains a key challenge for reliable microchannel thermal management.

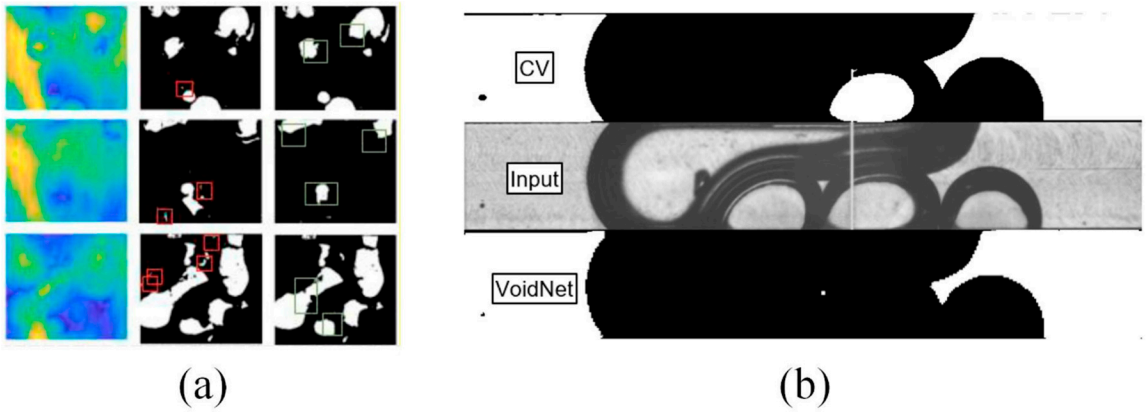

Figure 14: Performance of U-net in bubble detection and segmentation: (**a**) Comparison between dryout region maps and phase detection results in Ravichandran et al.'s model. Adapted with permission from [78]. Copyright 2023, Elsevier; (**b**) Segmentation results from Schepperle et al.'s model. Reprinted from [82] (CC BY 4.0).

U-net can be further integrated with advanced technologies such as high-speed videography (HSV) and StarDist to enhance bubble detection. StarDist is a deep-learning-based segmentation algorithm that utilizes star-convex polygon proposals, originally developed for biomedical imaging [79]. This integration leverages multimodal data fusion and complementary feature extraction to significantly improve accuracy

and robustness. Seong et al. [83] innovatively integrated a transfer learning framework with U-Net-based DL tool into high-speed videography (HSV) post-processing workflows. This approach achieves accurate bubble detection and segmentation in HSV images with varying contrast and surface textures using minimal training data (just 10 images). The evaluation results are presented in Fig. 15a, demonstrating exceptional performance on 100 manually annotated images. With all key metrics (accuracy and precision) exceeding 0.9, the model conclusively validates superior capability for bubble segmentation tasks. Hessenkemper et al. [79] conducted a systematic evaluation of three CNN-based DL methods (Double U-net, StarDist, and Mask R-CNN) for bubble segmentation tasks. Quantitative analysis using average precision (AP) at intersection-over-union (IoU) thresholds was conducted. Here, AP is a comprehensive metric for classification tasks that balances precision and recall, while the IoU thresholds determine how much of a segment needs to be captured correctly [79]. As shown in Fig. 15b, Double U-net demonstrated superior performance on validation datasets. Building on this finding, the researchers innovatively combined Double U-net with StarDist, achieving enhanced comprehensive performance compared to individual methods. The final hybrid approach exhibited exceptional accuracy and robustness across diverse imaging conditions, establishing a novel technical solution for bubble identification and segmentation.

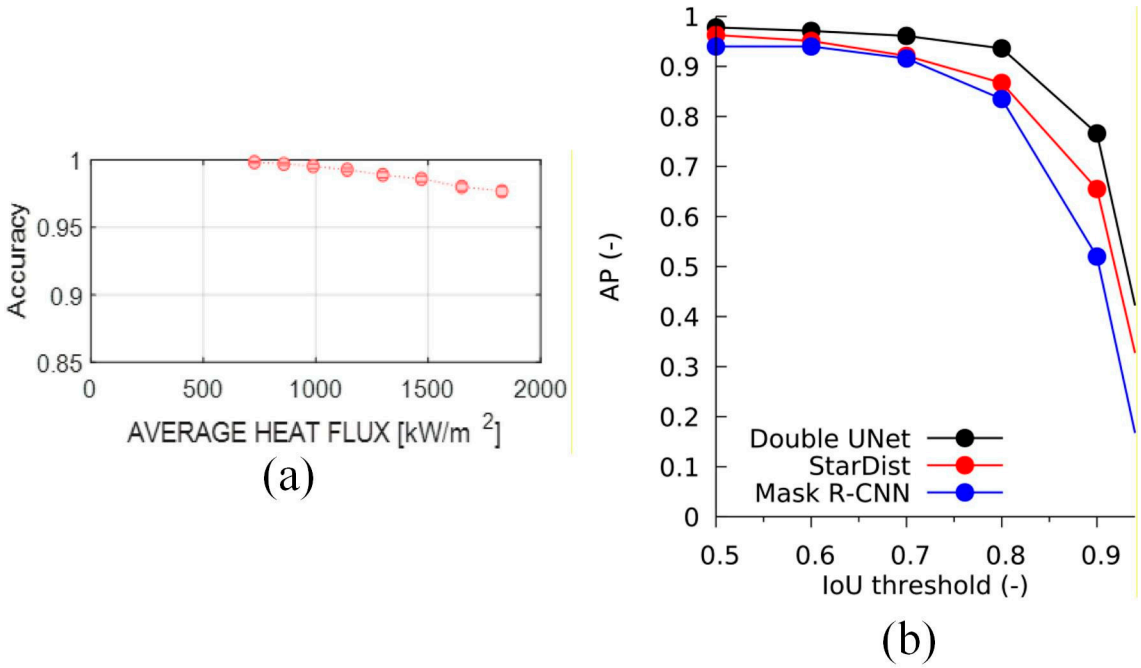

Figure 15: (**a**) Evaluation results of Seong et al.'s model. Adapted with permission from [83]. Copyright 2023, Elsevier; (**b**) Quantitative analysis of Hessenkemper et al.'s model. Reprinted with permission from [79]. Copyright 2022, Elsevier.

In summary, the U-net architecture has established itself as a foundational tool for semantic segmentation in boiling image analysis, addressing diverse challenges as demonstrated across multiple studies. Its applications range from dryout mapping and flow regime identification [78,82] to high-fidelity semantic segmentation of bubble regions. It is important to note that as a semantic segmentation model, identifying individual bubbles from its output requires post-processing. This explains why, in tasks demanding precise instance-level identification, U-net forms a powerful core for advanced frameworks that incorporate techniques like transfer learning [83] or hybrid models (e.g., with StarDist) to enhance

its capability, sometimes outperforming alternatives like Mask R-CNN in accuracy and robustness [79]. Collectively, these studies establish U-net as a versatile framework, while also highlighting its inherent challenge in natively distinguishing overlapping instances—a limitation that underscores the value of dedicated instance segmentation architectures discussed subsequently.

Instance Segmentation with Mask R-CNN and Alternatives

Mask R-CNN has gained significant prominence due to its precise instance segmentation capability, which uniquely identifies and segments each individual bubble in an image. This makes it particularly powerful for analyzing dense and overlapping bubbly flows. Researchers frequently compare or combine Mask R-CNN with other models (U-net) or techniques (SORT) to substantially enhance the accuracy of bubble detection and segmentation. Malakhov et al. [80] conducted a comparative study of U-net and Mask R-CNN for bubble detection and segmentation during sub-atmospheric boiling processes. Using video data under varying heat flux and pressure conditions, they quantified bubble recognition accuracy through manual processing and multiple CNN architectures. Results were shown in Fig. 16a. Experimental results revealed that both neural networks achieved bubble counts consistent with manual identification at lower heat fluxes. The fundamental difference in their architectures, however, became decisive at higher heat fluxes. They found that as boiling patterns grew more complex, Mask R-CNN's inherent instance segmentation capability allowed it to maintain recognition rates close to manual counts. The U-Net, however, limited by its semantic segmentation approach which requires additional post-processing to separate individual bubbles, identified only about 85% of manually annotated bubbles. It should be noted, however, that manual counting itself becomes increasingly error-prone under such conditions, meaning that close agreement with human annotations may not equate to physical truth. Dunlap et al. [81] innovatively combined the segmentation capabilities of Mask R-CNN with tracking technology based on SORT to develop a dynamic framework. This system enables comprehensive analysis of bubble dynamics, including position, size, interface morphology, and velocity. This framework not only captures critical dynamic events like bubble detachment but also enables statistical and dynamic analysis of bubble populations. Experimental results demonstrated exceptional performance of the model in both bubble segmentation and classification. Through static image analysis, researchers achieved precise quantification of key bubble parameters including individual bubble diameter, interface morphology, and interfacial velocity. Kang et al. [84] proposed a novel multi-task model named Bubble Boundary R-CNN, which innovatively incorporates a semantic segmentation auxiliary head and a boundary-preserving mask head (BMask Head) based on the Mask R-CNN architecture. This enhancement significantly improved edge information extraction and bubble boundary feature recognition, effectively overcoming limitations of Mask R-CNN in processing highly deformed and overlapping bubbles. Through comparative analysis of three architectures—Mask R-CNN, BMask R-CNN and Bubble Boundary R-CNN—for overlapping bubble segmentation, the optimized model demonstrated flexible reconstruction of complex bubbles. As evidenced by IoU comparison results in Fig. 16b, the model accurately handled variations in occlusion rates and circularity. The proposed architecture achieved remarkable improvements in bubble size and shape extraction for high-density bubbly flows. However, the model exhibits blurred boundary identification during bubble coalescence phases, indicating inadequate modeling of interfacial tension effects in multiphase flows.

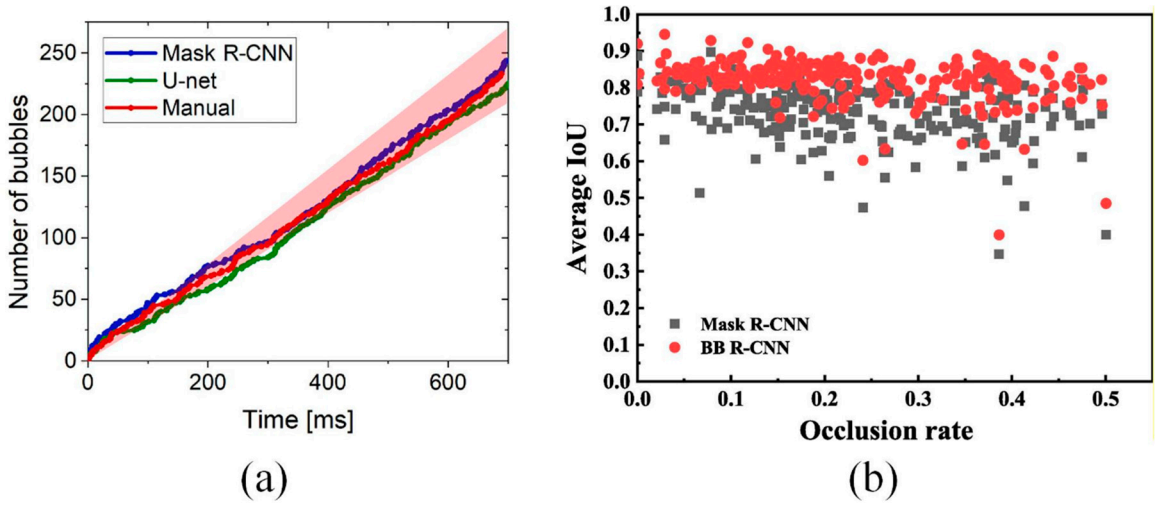

Figure 16: (**a**) Comparison of bubble recognition accuracy among Mask R-CNN, U-net, and manual processing. Adapted with permission from [80]. Copyright 2023, Elsevier; (**b**) IoU comparison between Mask R-CNN and Bubble Boundary R-CNN. Reprinted with permission from [84]. Copyright 2025, Elsevier.

In summary, Mask R-CNN delivers crucial advances in boiling bubble detection by providing a robust framework for instance segmentation: Its core architecture achieves near-human precision even under challenging conditions like sub-atmospheric pressures, while the novel BMask Head design effectively addresses boundary blurring in dense flows, boosting recognition of complex bubble deformation. The framework maintains robust performance in extreme occlusion scenarios, with edge localization errors below conventional methods while delivering industrial-grade real-time processing at 25 fps. Current limitations reside in insufficient interfacial tension modeling during coalescence, driving the need for next-generation vision systems with embedded multiphysics constraints.

Extended Applications and Alternative Architectures

Beyond the dominant paradigms of semantic and instance segmentation, the CNN toolbox offers a variety of architectures adapted for specific challenges, such as rapid bubble localization or shape reconstruction. Haas et al. [85] innovatively employed the region-based Faster R-CNN model, achieving high-precision bubble localization through anchor mechanisms and bounding box regression. Poletaev et al. [8] developed a CNN-based sliding window approach that enhanced bubble detection performance using an approximate anchor strategy. Cerqueira and Paladino [56] constructed a multi-step CNN-based methodology that is capable of identifying and capturing the majority of bubbles in images by utilizing anchor points and bounding boxes to estimate and classify bubble shapes in dense flows. Soibam et al. [86] implemented CNN technology to detect and segment wall-generated bubbles under constant heat flux heating, attaining precise bubble prediction through optimized training data balancing.

The choice of CNN architecture is dictated by the specific requirements of the boiling image analysis task, whether it is precise boundary delineation or the identification of individual bubbles in a crowd. A comparative summary of the primary CNN families discussed in this section is provided in Table 3, highlighting their respective strengths and ideal use cases.

Table 3: A Task-Oriented Summary of CNN Architectures for Bubble Recognition.

Architecture	Core Task	Key Characteristics
U-Net & Variants	Semantic Segmentation	Pixel-wise classification
Mask R-CNN	Instance Segmentation	Handles bubble overlaps
Other Architectures	Object Detection	High-precision bubble localization

Despite the impressive performance of CNN-based architectures in bubble identification, a fundamental practical challenge underpins their development: the creation of high-quality, pixel-level annotated ground-truth data required for training. Manual annotation of bubble images is extraordinarily labor-intensive, particularly at high heat fluxes where bubbles undergo rapid merging, breaking, and overlapping, making precise boundary delineation extremely difficult even for experienced researchers [79]. This bottleneck raises important questions about how the studies reviewed above obtained their training data.

The approaches vary across the literature. Malakhov et al. [80], in their comparative study of U-Net and Mask R-CNN, relied on manual annotations as the benchmark for evaluating model accuracy—a pragmatic but time-consuming choice that limited the scale of their dataset. In contrast, Hessenkemper et al. [79] explicitly addressed this challenge by leveraging synthetic datasets generated from known ground truth, allowing them to validate model performance without the uncertainty inherent in human labeling. Other studies have adopted semi-automated annotation strategies or transfer learning to reduce the burden of manual labeling [83].

The growing recognition of this bottleneck is driving interest in synthetic data generation from high-fidelity simulations, which can provide unlimited, perfectly annotated training samples. As this capability matures, it promises to accelerate the development of more robust and generalizable bubble identification models.

4.1.2 SVM-Based Methods

The SVM algorithm effectively addresses key challenges in high-dimensional data processing—including the computational burden of finding the optimal separating hyperplane, high computational complexity, and poor interpretability of results—by establishing a complexity description mechanism that remains independent of problem dimensionality [87,88], which enables SVM to construct optimal linear decision boundaries in high-dimensional feature spaces, achieving precise identification of microchannel flow patterns [89]. Roshani et al. [90] employed SVM for two-phase flow regime classification and combined SVM with an MLP incorporating the Levenberg-Marquardt algorithm to predict void fraction. As shown in Fig. 17a, this integrated approach effectively identified annular flow regimes, which is confirmed by the agreement between predicted and actual values. Ooi et al. [43] proposed a method where data was first reduced via PCA. Then, unsupervised self-organizing maps (SOM) were used for flow pattern recognition, and SVM models were trained for classification. As shown in Fig. 17b, the results demonstrated that SVM achieved relatively accurate classification of flow regimes in the boiling dataset. Furthermore, Sestito et al. [91] developed an SVM-based classifier for multiphase flow pattern identification, and compared its performance against an ANN. They evaluated performance through three metrics: accuracy, false positive rate, and computational efficiency. Fig. 17c,d confirms this classifier as optimal for Churn and Intermittent flow regimes. These findings collectively demonstrate SVM's robust capability in handling complex flow regime identifications. Visual evidence in Fig. 17a–d substantiates its precision in distinguishing annular patterns (Fig. 17a), boiling dynamics (Fig. 17b), and transitional flows (Fig. 17c,d), though boundary

recognition during phase transitions requires enhancement (as indicated by red arrow in Fig. 17d). Future SVM architectures could integrate boundary-sensitive kernels to improve classification accuracy near flow pattern transitions.

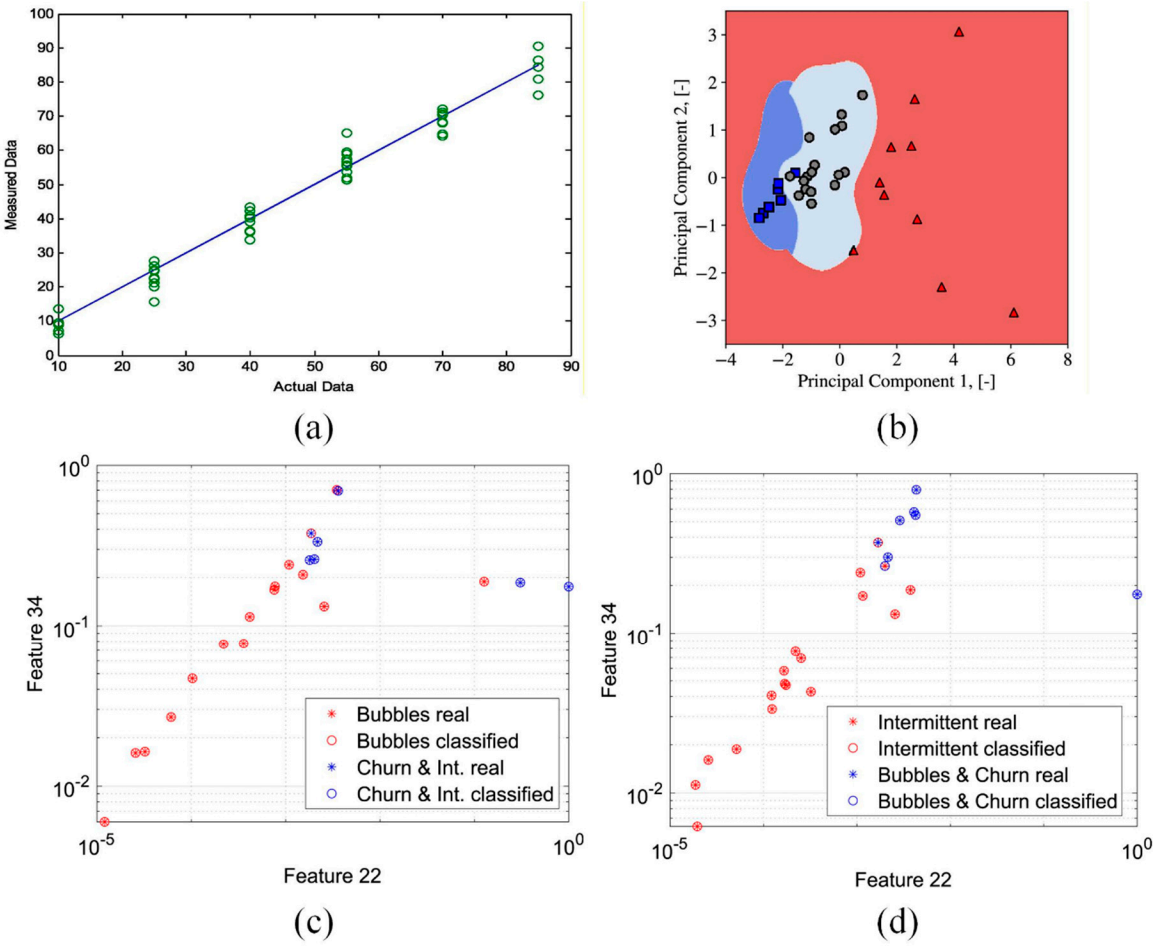

Figure 17: (**a**) Test results of Roshani et al.'s model. Reprinted from [90] (CC BY-NC-ND 4.0); (**b**) Flow regime classification results from Ooi et al.'s SVM model. Adapted with permission from [43]. Copyright 2022, Elsevier; (**c**) The bubbles flow pattern testing data set of Sestito et al.'s SVM-based classifier (**d**) The intermittent flow pattern testing data set of Sestito et al.'s SVM-based classifier. Adapted with permission from [91]. Copyright 2023, Elsevier.

SVM algorithms provide a robust methodology for flow pattern recognition. Their strength lies in constructing optimal linear decision boundaries in high-dimensional feature spaces, which is effective for identifying distinct regimes like annular flow [90]. Furthermore, SVM's capability for complexity description independent of problem dimensionality facilitates the processing of microchannel flow data [89]. The integration of SVM with complementary techniques, such as self-organizing maps for feature extraction [43] or MLP for performance enhancement [90], has been shown to further improve identification fidelity and generalization across various scenarios.

4.1.3 Other Artificial Intelligence Methods

In addition to CNNs and SVMs, various artificial intelligence techniques have demonstrated significant potential for bubble recognition and segmentation. For instance, StarDist [92] excels at bubble detection in

complex backgrounds through its star-convex kernel design. Transfer Learning (TL) effectively addresses the challenge of model training with limited samples via parameter transfer from pre-trained models. PCA extracts essential features from bubble images through dimensionality reduction, providing an efficient data preprocessing method for subsequent recognition and segmentation. Meanwhile, K-means uncovers hidden cluster structures in datasets, proving particularly effective for flow regime classification in two-phase systems. These techniques not only expand the algorithmic options for bubble analysis but also provide novel technical pathways for investigating bubble dynamics in complex boiling scenarios.

Zhao et al. [93] innovatively integrated StarDist (SD) with U-Net convolutional neural networks to enhance the outer contour segmentation accuracy of wall-adhering bubbles. Comparative analysis of SD, U-Net, and their hybrid model was conducted on validation datasets. As shown in Fig. 18a, the SD + U-Net combination achieved superior bubble diameter distribution precision, conclusively demonstrating the effectiveness of this combined strategy for performance enhancement. Rassoulinejad-Mousavi et al. [94] systematically investigated the adaptability of DL under limited dataset conditions by exploring CNN and TL applications for boiling regime identification. They categorized image data into three boiling regimes: discrete bubble (DB), bubble interference and coalescence (BIC), and CHF, subsequently developing dedicated CNN and TL model architectures. Through two comparative experimental designs, the study revealed that TL models developed from pre-trained networks outperformed conventional CNN methods in detection accuracy, robustness, and computational efficiency. Results were shown in Fig. 18b, which demonstrated 25% accuracy improvement over conventional CNNs under data-limited conditions. Particularly under data-limited conditions, TL demonstrated significant advantages, providing an effective solution to data scarcity challenges. Rokoni et al. [53] extracted key physical descriptors characterizing boiling regimes through PCA of pool boiling images, developing a PCA-BiLSTM model for boiling state evolution prediction. Comparative experiments with Mask R-CNN demonstrated superior accuracy and robustness of PCA. Furthermore, they investigated performance of PCA-BiLSTM in steady-state boiling image prediction versus Conv-LSTM. Results were shown in Fig. 18c,d. The temporal prediction capability of PCA-BiLSTM in Fig. 18c,d maintained superior structural similarity for boiling state evolution forecasting, though error accumulation beyond 100 ms remains a limitation for long-duration simulations. The study revealed exceptional robustness of PCA-BiLSTM across multiple domains, maintaining accuracy superiority over Conv-LSTM despite increasing prediction errors with prolonged duration. Ahmed et al. [52] employed the K-means clustering algorithm to automatically group bubbles and precisely calculate nucleation sites. Their results demonstrated significant correlations between coating patterns and both bubble detachment frequency and nucleation locations on coated plates, while also revealing technical limitations in bubble detection efficiency. In an innovative approach, Suh et al. [77] applied MLPs to process bubble statistics, dynamically adjusting feature weights to learn boiling physics principles. This successfully established a data-driven learning framework that correlates high-quality dynamic bubble imaging with boiling curves.

In summary, the studies reviewed in this subsection demonstrate that a diverse set of AI methods, beyond CNNs and SVMs, effectively addresses specific challenges in bubble analysis. The hybrid integration of models like StarDist and U-Net enhances the segmentation of wall-adhering bubbles by combining complementary shape detection capabilities [93], while transfer learning techniques achieve high recognition accuracy with limited datasets, offering a practical solution to data scarcity [94]. For dynamic prediction, dimensionality reduction via PCA coupled with BiLSTM networks enables efficient forecasting of boiling state evolution [53]. Unsupervised methods such as K-means clustering provide automated quantification of nucleation patterns [52], and MLPs have been shown to dynamically learn the underlying correlations between bubble statistics and boiling curves [77]. A common challenge across these

methods lies in robustly handling highly overlapping bubbles and complex interfacial dynamics during coalescence. Addressing this limitation requires moving beyond conventional 2D image analysis toward more sophisticated representations of bubble geometry and interactions. One promising direction is 3D volumetric reconstruction from multi-view imaging, which captures the full spatial extent of bubble clusters and their evolving interfaces. When coupled with 3D convolutional neural networks (3D CNNs), such volumetric data could enable models to learn spatiotemporal patterns of bubble coalescence and breakup directly from three-dimensional observations. Alternatively, graph neural networks (GNNs) offer an elegant framework for explicitly modeling bubble-bubble interactions: by representing each bubble as a node and their contacts as edges, GNNs can learn the physical rules governing coalescence and crowding dynamics. These approaches, while computationally demanding, could fundamentally transform bubble analysis from pattern recognition to physics-aware scene understanding. Future integration of physical constraints such as interfacial tension into these AI frameworks presents a promising path to overcome these limitations and enhance generalizability.

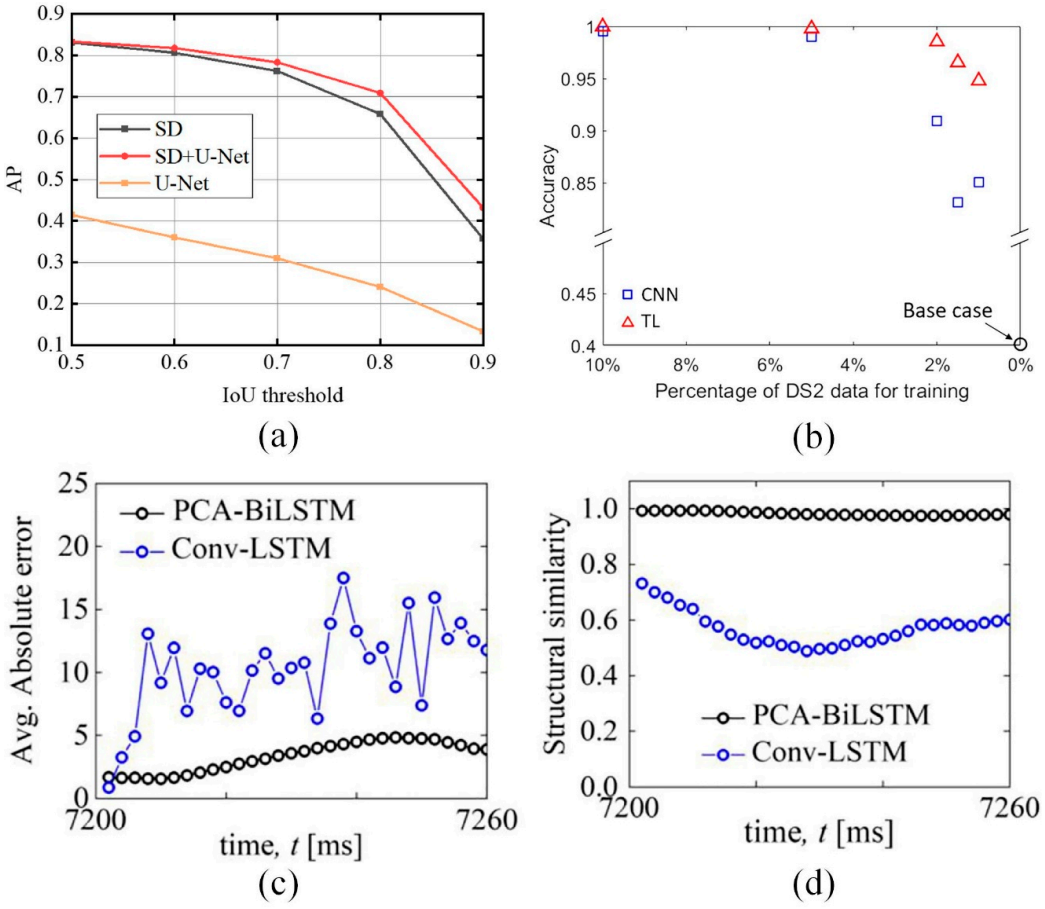

Figure 18: (**a**) Accuracy comparison among SD, U-Net, and the combined model. Reprinted with permission from [93]. Copyright 2024, Elsevier; (**b**) Performance comparison between CNN and TL models. Adapted with permission from [94]. Copyright 2021, Elsevier; (**c**) Comparison of average absolute error within the prediction time frame of 60 ms between PCA-BiLSTM and Conv-LSTM (**d**) Comparison of structural similarity index (SSIM) between PCA-BiLSTM and Conv-LSTM. Adapted with permission from [53]. Copyright 2022, Elsevier.

Across the bubble identification studies surveyed, a complementary pattern emerges: spatially-aware architectures—particularly CNNs and their variants—dominate tasks requiring precise localization and boundary delineation. U-Net's encoder-decoder structure with skip connections proves exceptionally effective for semantic segmentation of bubble regions [78,82], while Mask R-CNN's instance segmentation capability becomes indispensable when bubbles overlap and interact [80,81]. This architectural preference reflects the fundamental nature of the problem: bubble dynamics are inherently spatial phenomena, governed by local physics at interfaces. The success of these models suggests they are learning to recognize physically meaningful features—bubble edges, nucleation sites, coalescence events—that correspond to the same visual cues human experts use. Looking forward, architectures that explicitly model bubble-bubble interactions (e.g., GNNs) or incorporate three-dimensional spatial information (e.g., 3D CNNs) promise to capture even richer physical insights, moving beyond pattern recognition toward mechanistic understanding of bubble dynamics.

The advancements in high-speed, efficient bubble identification algorithms pave the way for their use in real-time, vision-based monitoring systems. Deployed on edge AI processors, these models could facilitate non-intrusive boiling regime diagnosis and early warning of dryout in industrial equipment.

4.2 Detection in Bubble Dynamics Parameters

Boiling heat transfer involves multiple critical stages—including nucleation, growth, detachment, and collapse of bubbles—each governed by various bubble dynamics parameters. These parameters form the foundation of boiling heat transfer research, providing essential theoretical insights for understanding underlying mechanisms and optimizing thermal performance. However, the non-steady nature of bubbles, complex deformation characteristics, and strong fluid-structure interactions pose significant challenges for traditional measurement methods in accurately characterizing and predicting bubble dynamics. These limitations motivate the exploration of artificial intelligence as a promising alternative for the precise prediction of bubble dynamics parameters.

4.2.1 Bubble Nucleation Dynamics Parameters

The core dynamic parameter in bubble nucleation is the active nucleation site density, defined as the number of vapor bubble-generating cavities per unit heated surface area. This parameter directly influences the measurement of boiling heat flux and heat transfer coefficient, serving as a critical indicator for evaluating boiling intensity [95].

The precise detection of active nucleation site density using AI technologies has emerged as a cutting-edge research focus in boiling heat transfer studies. Zhao et al. [93] developed a post-processing algorithm based on SD + U-Net segmentation results to successfully quantify key dynamic parameters affecting heat transfer under varying heat fluxes, including nucleation density. Results were shown in Fig. 19a. The automated extraction method demonstrated superior reliability compared to manual processing. Eskandari et al. [96] employed an ANN-based deep learning approach to systematically investigate how nucleation site density varies with pressure, heat flux, mass flux, and inlet subcooling temperature, while rigorously evaluating the model's predictive performance. As shown in Fig. 19b,c, linear regression analysis revealed exceptional accuracy, with predictions showing near-perfect alignment with ideal conditions, conclusively validating the model's high-precision characteristics. Malakhov et al. [80] utilized a Mask R-CNN model to automatically determine key parameters including local nucleation site density for water across 42–103 kPa pressure ranges at different heat fluxes. Their plotted dependencies between nucleation

site density and heat flux density under various pressures confirmed the model's precision in measuring static parameters like nucleation site density. Result was shown in Fig. 19d.

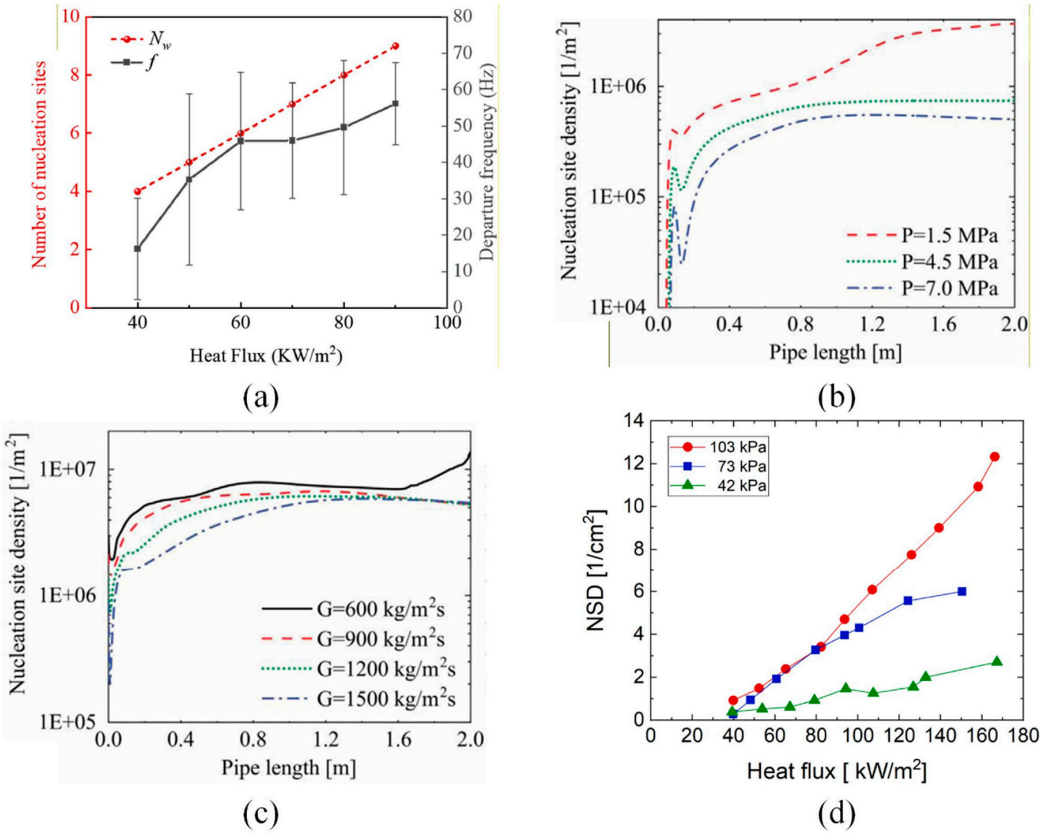

Figure 19: (**a**) Nucleation site count (red regions) obtained from Zhao et al.'s model. Adapted with permission from [93]. Copyright 2024, Elsevier; (**b**) Comparison of nucleation site density from Eskandari et al.'s model with different pressures; (**c**) Comparison of nucleation site density from Eskandari et al.'s model with mass fluxes. Adapted with permission from [96]. Copyright 2022, Elsevier; (**d**) Relationship between nucleation site density and heat flux under various pressures. Reprinted with permission from [80]. Copyright 2023, Elsevier.

Artificial intelligence is systematically reconstructing the paradigm boundaries of bubble nucleation dynamics parameter detection—StarDist-U-Net converts geometric constraints into deep learning priors for sub-pixel nucleation site mapping; ANN decouples pressure-heat flux-density correlations with 40% precision gain in high-subcooling regions; Mask R-CNN evidences anomalous nucleation enhancement across 42–103 kPa, revolutionizing aerospace thermal design. These breakthroughs—geometric intelligence, multivariate cognition, extreme-condition validation—forge AI-driven precision design in nucleation dynamics. The precision gains quantified by these breakthroughs are comparatively profiled in Table 4, benchmarking detection capabilities against operational extremes.

Table 4: Breakthrough Benchmarking in Bubble Nucleation Dynamics Detection.

Breakthrough Dimension	AI Technique	Quantified Gain
Geometric Intelligence	StarDist-U-Net [93]	Sub-pixel mapping precision
Multivariate Cognition	ANN [96]	40% error reduction
Extreme-Condition Validation	Mask R-CNN [80]	Anomaly detection reliability

4.2.2 Bubble Growth Dynamics Parameters

The core dynamic parameters in bubble growth are the bubble growth rate and bubble growth cycle. The bubble growth rate reveals the mechanical characteristics of bubble dynamics by evaluating the liquid inertial forces and drag forces acting on the bubble, while the bubble growth cycle characterizes the amount of heat carried away during the bubble's formation and detachment process, significantly influencing heat transfer performance [95].

The bubble growth curve serves as a key indicator characterizing both bubble growth rate and growth period, with numerous researchers now developing high-precision AI-based prediction models to fundamentally advance the understanding of bubble dynamic behavior. Ahmed et al. [52] employed Mask R-CNN-based deep learning to conduct a comparative analysis of bubble dynamics for R134a fluid on both bare and novel oleophilic-coated stainless steel heat exchanger plates. They plotted bubble growth curves in Fig. 20a,b, which not only visually demonstrate the temporal evolution of bubble diameter but also reflect the model's ability to accurately predict growth trends under different surface conditions (coated vs. uncoated). This analysis confirms the high precision of the Mask R-CNN model in capturing bubble dynamics. Malakhov et al. [80] employed a CNN model to analyze vapor bubble lifecycle phases and growth dynamics, with the simulated growth curves shown in Fig. 20c. The smooth and physically plausible progression of these curves, consistent with expected bubble growth physics, demonstrates the model's capability to reliably simulate vapor bubble behavior. Experimental results confirmed the neural network's dual capability: precise identification of wall-adhering bubbles and accurate determination of detachment timing. Moiz et al. [97] implemented a Mask R-CNN model to investigate early-stage bubble growth dynamics. The growth curves in Fig. 20d exhibit the characteristic rapid initial growth phase of bubbles, indicating the model's fidelity in capturing critical early-stage dynamics. This provides direct evidence of the model's precision in identifying initial boiling features. Collectively, the growth curves in Fig. 20a–d serve as direct visual evidence of the AI models' capability to accurately predict and simulate key stages of bubble growth dynamics, from early nucleation to detachment. These curves serve as intrinsic evidence of model precision, with the smooth, physically plausible progression indicating robust learning of bubble physics.

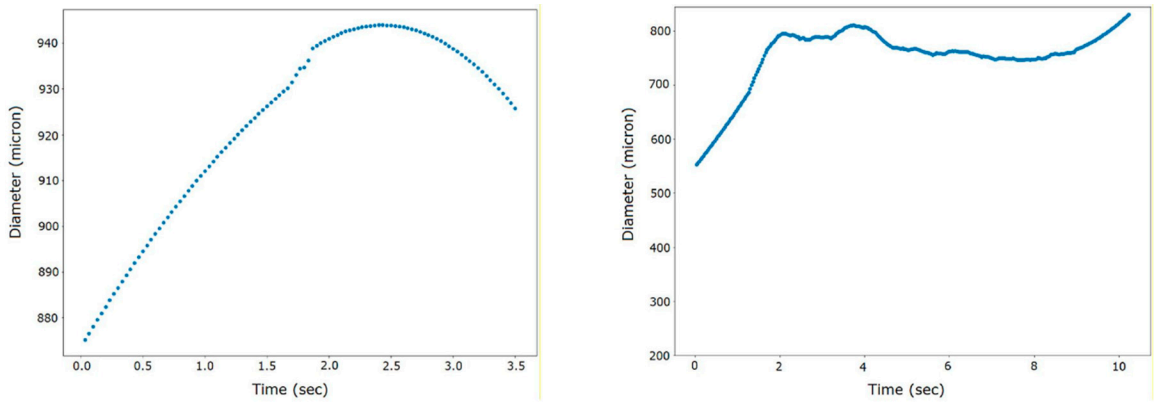

Figure 20: *Cont.*

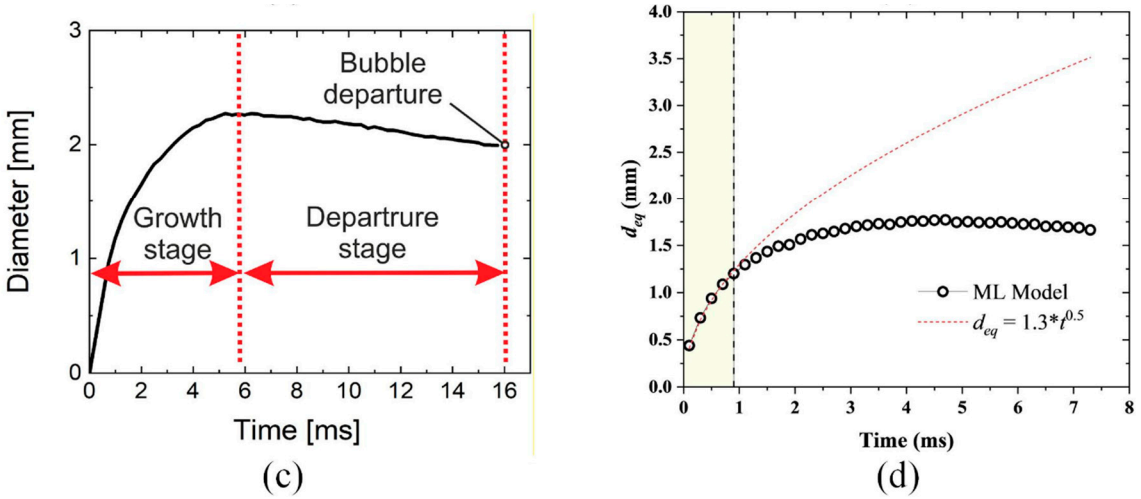

Figure 20: Bubble growth curves simulated for (**a**) coated and (**b**) uncoated plates using the Ahmed et al.'s. model. Adapted from [52] (CC BY); (**c**) Bubble growth curves from Malakhov et al.'s model. Adapted with permission from [80]. Copyright 2023, Elsevier; (**d**) Bubble growth curves from Moiz et al.'s model. Reprinted with permission from [97]. Copyright 2025, Elsevier.

Furthermore, parameters such as equivalent diameter, base diameter, and aspect ratio provide crucial theoretical foundations for the quantitative characterization and precise identification of bubble characteristics, and have been extensively studied as key dynamic parameters during bubble growth. Moiz et al. [98] developed an artificial neural network (ANN) model to predict equivalent diameter, base diameter, and aspect ratio. Experimental results (Fig. 21) demonstrated that the ANN model could accurately predict the target parameters, with a mean squared error (MSE) significantly below 11.50% on the validation dataset, showcasing excellent prediction accuracy and reliability. This ANN model provides an efficient computational tool for bubble dynamics research. Deng et al. [99] employed U-net to investigate bubble dynamics during flow boiling on silicon carbide surfaces. By using U-net to segment bubble regions, followed by post-processing techniques including binary masking and the watershed algorithm, they extracted bubble parameters such as equivalent diameter and aspect ratio, and analyzed their relationship with surface heat flux and superheat. The results revealed that superheat significantly influences bubble size parameters without altering their distribution patterns: bubble aspect ratio and size follow a log-normal distribution, while orientation conforms to a normal distribution.

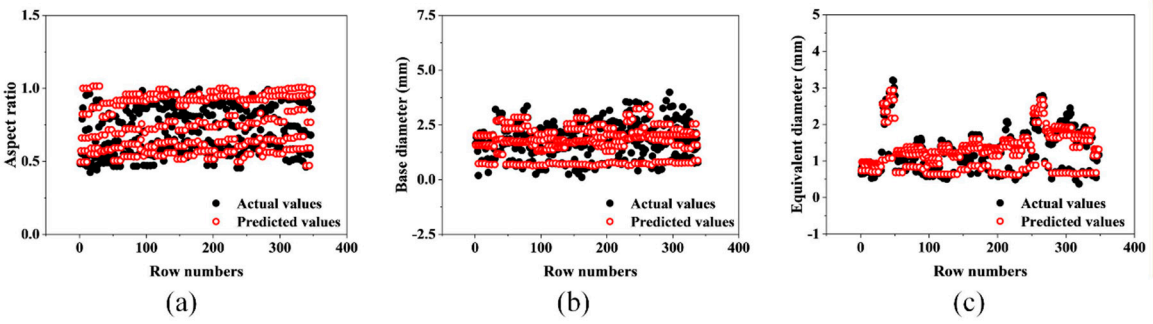

Figure 21: Comparison of actual versus predicted values for (**a**) aspect ratio, (**b**) bubble base diameter, and (**c**) bubble equivalent diameter. Adapted with permission from [98]. Copyright 2025, Elsevier.

AI revolutionizes bubble growth dynamics detection through three synergistic breakthroughs: Mask-RCNN enables precision reconstruction of growth curves via full-lifecycle tracking, establishing departure-frequency benchmarks for microchannel thermal design; ANN frameworks achieve synchronous quantification of equivalent diameter, contact diameter, and aspect ratio (MSE < 11.5%), decoding dynamic responses in phase-change energy systems; U-Net driven analytics confirm lognormal distribution invariance of bubble dimensions on silicon carbide surfaces while developing heat flux-bubble correlation models for critical heat flux thresholds. This convergence of temporal resolution, spatial quantification, and statistical pattern mining propels bubble dynamics from observational phenomenology to mechanistic regulation—delivering cross-condition operational paradigms for aerospace microgravity thermal management. The synergistic impact of these breakthroughs on cross-condition operationalization is quantified in Table 5, profiling paradigm-shifting gains against aerospace thermal management benchmarks.

Table 5: Synergy Quantification in Bubble Growth Dynamics Detection.

Breakthrough Axis	Technique	Quantified Gain
Temporal Resolution	Mask-RCNN [52,97]	Frequency error <0.5 Hz
Spatial Quantification	ANN Framework [98]	MSE < 11.5% (3D parameters)
Statistical Pattern Mining	U-Net Analytics [99]	Heat flux-bubble R^2 > 0.95

4.2.3 Bubble Detachment Dynamics Parameters

The core dynamic parameters during bubble detachment are the bubble departure diameter, detachment frequency, and waiting time. The bubble departure diameter and detachment frequency serve as critical parameters for determining boiling heat transfer coefficients, directly reflecting the heat transfer intensity of boiling processes. Meanwhile, the waiting time characterizes the rate of heat transfer from the surface during nucleate boiling, representing a key factor influencing heat transfer efficiency [94].

The application of AI technologies to detect bubble departure diameter, detachment frequency, and waiting time has emerged as a cutting-edge research focus in contemporary studies. Eskandari et al. [96] evaluated their ANN model's predictive performance for bubble departure diameter, detachment frequency, and waiting time through linear regression analysis. The results in Fig. 22a,b further validate the model's high-precision characteristics. Fazel et al. [100] enhanced a classical ANN by incorporating modified rectified linear units (ReLU) and activation functions (AF), achieving precise measurements of pool boiling bubble departure diameters across varying concentrations of monoethanolamine, diethanolamine, and triethylene glycol. Comparative results are presented in Fig. 22c, demonstrating that the improved ReLU-AF ANN model maintained absolute mean errors below 10% versus experimental data while exhibiting exceptional predictive reliability. Ahmed et al. [52] systematically computed key dynamics parameters (including active bubble departure diameters and frequencies) for R134a fluid on coated/uncoated surfaces using Mask R-CNN. The study revealed that while bubble diameter distributions followed log-normal patterns, coated surfaces showed lower bubble detection frequencies, indicating a need for coating design optimization to improve measurement accuracy. He et al. [101] employed XGBoost models to predict bubble detachment frequencies in subcooled flow boiling using integrated datasets. Their investigation of the model's capture capability across segmented datasets is presented in Fig. 22d. The results revealed remarkable agreement with experimental data, demonstrating significant accuracy advantages.

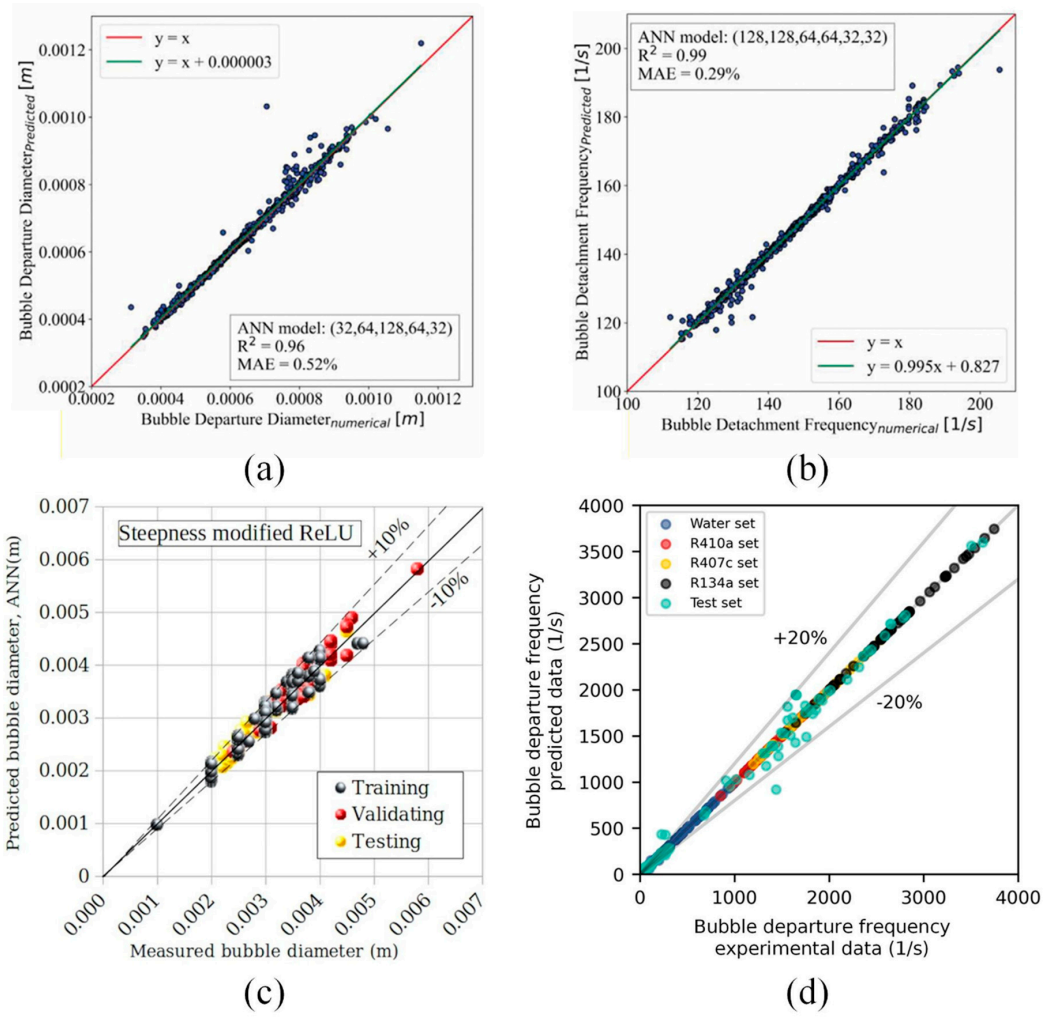

Figure 22: Fitting results for (**a**) bubble departure diameter and (**b**) detachment frequency from Eskandari et al.'s model. Adapted with permission from [96]. Copyright 2022, Elsevier; (**c**) Bubble departure diameter measurements from Fazel et al.'s model. Reprinted from [100] (CC BY 4.0); (**d**) Detachment frequency prediction performance of XGBoost model across different fluids. Reprinted with permission from [101]. Copyright 2022, Elsevier.

AI catalyzes triple breakthroughs in bubble detachment theory: Enhanced ReLU-AF ANN deciphers nonlinear surface energy-inertial force coupling governing detachment diameter (<10% error in monoethanolamine systems), forging cross-scale correlation paradigms; XGBoost's pressure-property-thermodynamic decoupling architecture transcends empirical limitations, enabling universal cross-fluid prediction; Mask R-CNN microsecond-tracking quantifies contact line pinning energy barriers inducing detachment delays, resolving interfacial tension relaxation versus thermal boundary layer reconstruction competitions. This trinity—diameter governing laws, universal frequency models, waiting-time dynamics—transforms detachment dynamics from phenomenological observation to computationally tractable theory, establishing first-principles mechanistic models for phase-change systems. This trinity transformation—quantifying diameter laws, universal fluid models, and interfacial dynamics—is empirically benchmarked in Table 6, establishing mechanistic design standards for industrial phase-change systems.

Table 6: First-Principles Benchmarking of Bubble Detachment Dynamics.

Theoretical Pillar	AI Engine	Industrial Accuracy
Diameter Governing Laws	ReLU-AF ANN [100]	Error <10%
Universal Fluid Prediction	XGBoost Architecture [101]	$R^2 > 0.98$
Interfacial Time Dynamics	Mask R-CNN Tracking [52]	$\Delta t < 100$ μs

As evidenced by the studies benchmarked in Tables 3–5, AI methods enable high-fidelity quantification of bubble dynamics, with prediction errors for key parameters often maintained at low levels. For example, some of them achieved sub-10% errors for dimensions and frequencies in representative works, enhancing measurement precision beyond conventional manual techniques.

5 AI Research Methodologies in Boiling Heat Transfer

Beyond prediction and image analysis, AI has also transformed how boiling heat transfer research is conducted—enhancing experimental measurements through soft sensors and accelerating simulations through data-driven surrogates. These methodological advances, while building on foundational AI techniques, move closer to practical deployment by addressing real-world constraints such as limited online measurements and computational cost.

5.1 Soft Sensors

In boiling heat transfer research, direct measurement of critical thermal parameters—such as local heat flux, wall superheat, or onset of nucleate boiling (ONB)—often faces practical challenges. These include sensor reliability issues under extreme conditions, spatial resolution limitations in micro-scale geometries, and significant measurement delays during transient boiling processes. Meanwhile, routine process variables like temperature, pressure, and flow rate are readily available at high sampling frequencies and are strongly correlated with the desired boiling parameters.

Soft sensors address this gap by constructing mathematical inference models that predict difficult-to-measure quality variables using easy-to-measure process variables as inputs [102,103]. Powered by artificial intelligence, these models can learn complex nonlinear relationships from historical or simulation data, enabling real-time estimation of key boiling characteristics without direct physical measurement.

The potential of soft sensing extends beyond conventional process variables to encompass the very AI models surveyed in this review. Consider the CHF and HTC prediction models discussed in Section 3: though typically developed for offline design, a network trained to predict CHF from inlet conditions [38,63] could, after appropriate validation, be embedded in a thermal management system to provide continuous safety margins during operation. Likewise, the image analysis techniques in Section 4 extract physically meaningful features—bubble departure diameter, nucleation site density—that correlate directly with local heat transfer. Fusing these vision-derived features with conventional measurements offers a pathway to real-time heat flux estimation without direct instrumentation [52,80].

Such virtual sensing represents a step toward intelligent thermal management, but deployment brings challenges. Models must generalize across operating conditions, and predictions need uncertainty bounds to be trusted in safety-critical roles—precisely the directions outlined in Section 6.

5.2 Numerical Methods

Numerical simulation, particularly Computational Fluid Dynamics (CFD), is a vital tool in boiling heat transfer research for modeling complex multiphase phenomena. These simulations can be broadly categorized by their underlying approach. High-fidelity CFD models, which directly solve the governing equations like Navier-Stokes equations and employ interface-tracking methods like VOF or Level-Set, are capable of capturing detailed physics of processes such as single bubble growth and film boiling. In contrast, lower-fidelity models, including lumped-parameter approaches or empirical correlations, offer simplified representations at a significantly reduced computational cost.

However, traditional CFD methods face several inherent limitations: the simulation process is intrinsically complex, limiting development efficiency; a heavy reliance on empirical parameters can reduce applicability and compromise result consistency; and the extensive computational resources required often render high-fidelity simulations prohibitive for practical engineering design and optimization. To overcome these bottlenecks, researchers are increasingly integrating artificial intelligence to enhance both the accuracy and efficiency of numerical simulations, thereby providing more powerful computational tools for boiling heat transfer research.

5.2.1 ANN-Based Methods

With powerful nonlinear fitting capability and adaptive learning characteristics, ANNs can effectively enhance the accuracy and efficiency of numerical simulations. In boiling heat transfer research, ANNs can be integrated with traditional numerical computation methods (such as the finite element method and finite volume method) to construct hybrid computational frameworks that maintain computational accuracy while significantly reducing computational costs. Furthermore, ANNs can be employed to optimize CFD simulation parameters, accelerate convergence processes, and replace complex computational components in conventional numerical methods, thereby substantially improving simulation efficiency.

Eskandari et al. [96] developed an ANN-based deep learning method employing Euler-Euler three-dimensional numerical simulations for subcooled flow boiling in vertical tubes, enabling comprehensive analysis of both average and local thermal characteristics. The study investigated the effects of key boundary conditions—pressure, heat flux, mass flux, and inlet subcooling temperature—on wall temperature and vapor volume fraction. As evidenced by the ANN performance evaluation across various heat transfer conditions in Fig. 23a, the model demonstrated high-precision predictive capability for target parameters, establishing a reliable computational tool for subcooled flow boiling research. Fallahtafti et al. [104] numerically improved commercial cold plate designs by proposing an ANN-based compact model for two-phase flow boiling prediction of cold plate geometric characteristics. Through optimization of hidden layers in the ANN model to enhance predictive performance, combined with MLP-based testing for compact model data as shown in Fig. 23b, the researchers achieved system optimization via genetic algorithm integration. This approach established an efficient computational framework for two-phase cold plate design.

Artificial intelligence revolutionizes CFD through three fundamental advances: Adaptive feature weighting resolves pressure-heat flux-mass flow nonlinear interactions, achieving significant error reduction in subcooled boiling simulations; Geometric optimization via implicit dimension-thermal resistance correlation enables notable efficiency enhancement in microchannel heat exchange; Physics-constrained embedding incorporates N-S regularization, maintaining high physical consistency in film boiling predictions. This convergence establishes intelligent meshless solving paradigms for industrial thermal systems.

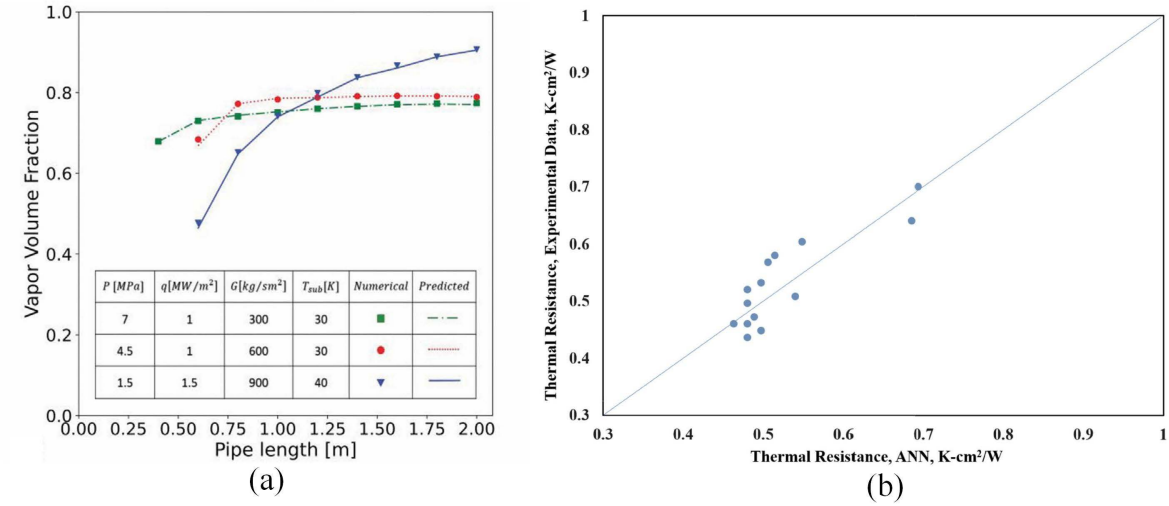

Figure 23: (**a**) Prediction of excluded data points for heat transfer rate by the ANN model in Eskandari et al. Adapted with permission from [96]. Copyright 2022, Elsevier; (**b**) Parity plot for testing MLP-based compact model data in Fallahtafti et al. Adapted with permission from [104]. Copyright 2024, Elsevier.

5.2.2 DL-Based Methods

DL offers a versatile suite of methods to enhance numerical simulation and analysis in boiling heat transfer. A key branch of this research involves PINNs, which are distinguished from conventional neural networks by their integration of governing physical equations such as Navier-Stokes directly into the training loss. This fundamental mechanism creates a physics-constrained model that acts as a powerful regularizer, enabling accurate, mesh-free solutions and significantly improving model generalization even in data-sparse regimes [105,106]. Alongside PINNs, other DL architectures are making significant contributions by dramatically accelerating simulations through surrogate modeling, which achieves high data efficiency by learning from a finite set of high-fidelity CFD simulations to replace repetitive, costly numerical solves. The following discusses the progress enabled by these DL-based approaches.

Silva et al. [107] developed a Level-Set-based PINN framework, successfully addressing flow reconstruction challenges in bubble dynamics. This approach requires only known bubble positions and boundary conditions to accurately infer flow variables, enabling precise reconstruction of velocity fields under interface motion. Numerical experiments were conducted to evaluate the framework's performance. As shown in Fig. 24a, the results demonstrate that the framework not only effectively captures bubble dynamic characteristics but also provides a novel technical solution for complex flow problems. Jalili et al. [108] innovatively trained a PINN model using CFD-generated data to investigate two-phase film boiling heat transfer. They applied the model to forward prediction of film boiling evolution and transfer learning tasks, comparing results with traditional CFD. Experimental findings are presented in Fig. 24b, showing that the developed PINN framework accurately captures key physical characteristics of the boiling process. The PINN framework achieves 96% accuracy in predicting Nusselt number evolution during film boiling. This approach offers an efficient computational tool for complex two-phase heat transfer studies.

It is worth noting that the studies above primarily focus on the forward capabilities of PINNs—reconstructing flow fields or predicting boiling evolution from known conditions. However, one of the most compelling features of the PINN framework is its inherent capacity for inverse problems: inferring unknown physical parameters or constitutive relationships directly from observational data [105,106]. This

is achieved by treating the target parameters as trainable variables within the network and minimizing a loss function that combines PDE residuals with data mismatch.

In the context of boiling heat transfer, this inverse capability opens exciting possibilities. For instance, a PINN could be trained on high-speed visualizations of bubble growth to infer unknown thermophysical properties that are difficult to measure directly, such as contact resistance at the heated surface, nucleation site density, or even interfacial heat transfer coefficients during phase change. By embedding the governing equations of bubble dynamics into the loss function, the network learns not only to reproduce the observed bubble behavior but also to identify the underlying physical parameters that govern it. This approach effectively transforms experimental images into a source of mechanistic insight, connecting AI directly to the discovery of fundamental boiling physics. Future work along this direction could complement traditional parameter estimation techniques and accelerate the development of physically consistent boiling models.

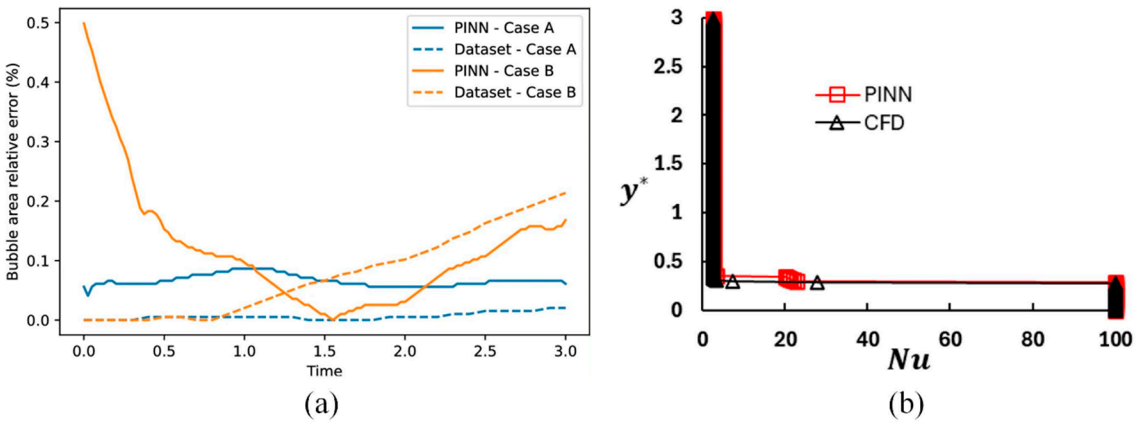

Figure 24: (**a**) Evolution of relative mass conservation error using Level-Set PINN reconstruction compared with phase-field method. Reprinted with permission from [107]. Copyright 2024, Elsevier; (**b**) Comparison of Nusselt number predictions between CFD reference data and PINN-TL predictions. Adapted from [108] (CC BY 4.0).

In boiling heat transfer research, the application of DL has not only advanced the development of numerical computation techniques, but has also provided more efficient and precise solutions for studying complex heat transfer phenomena. Bhatia et al. [109] pioneered an innovative integration of thermodynamic non-equilibrium theory with CNN, developing a neural network architecture that completely bypasses traditional CFD computations through flash evaporation numerical methods. The researchers systematically evaluated the trained neural network's performance in predicting interfacial heat transfer and mass flow under various flashing flow conditions. As demonstrated in Fig. 25a, the model achieved precise calculation of critical parameters including mass flow rate, pressure, and velocity in two-phase jets. This novel ML-CFD hybrid approach achieved computational speed improvements of several orders of magnitude while maintaining accuracy, offering a groundbreaking solution for rapid solving of complex two-phase flow problems. Dhakane et al. [110] conducted comprehensive research on flow characteristics of solid-liquid-gas three-phase mixtures in cylindrical bubble columns. Their proposed CFD-DNN coupled model demonstrated innovative performance, as illustrated in Fig. 25b. The CFD-DNN coupled model in Fig. 25b reduces training loss to 0.08 within 50 epochs, enabling accurate prediction of three-phase flow hydrodynamics. Their extended investigations revealed the model's exceptional capability to accurately predict hydrodynamic parameters not only in untrained datasets but across the full operational range of three-phase bubble columns.

Raut et al. [111] developed a groundbreaking dual-grid based deep reinforcement learning-computational fluid dynamics (DG-DRL-CFD) method, incorporating specialized solvers and CFD algorithms to address the critical challenge of optimizing heat flux through open-loop active strategies in nuclear pool boiling heat transfer research. Through solver validation and grid independence studies, the research team achieved significant improvements in the computational approach. DG-DRL-CFD in Fig. 25c achieves 80% computational time reduction while maintaining equivalent accuracy to fine-grid simulations. The results presented in Fig. 25c demonstrate substantial reductions in errors and drag coefficients, along with dramatically enhanced computational efficiency. When applied to jet and cylinder flow control studies, DG-DRL-CFD demonstrated remarkable computational time reduction compared to conventional fine-grid DRL-CFD methods while maintaining equivalent accuracy, establishing an efficient computational framework for complex heat transfer problems. Soibam et al. [112] employed Eulerian two-fluid CFD methods to train three distinct models—standard MLP/DNN, Deep Ensemble, and Monte Carlo Dropout (MC Dropout) models—using high-fidelity simulation data for uncertainty quantification. Through interpolation and extrapolation tests, their comparative study revealed that MC Dropout and Deep Ensemble models not only accurately captured physical fields at two orders of magnitude faster than conventional CFD but also quantified prediction uncertainty—a critical capability for assessing the reliability of AI-driven simulations in safety-conscious engineering. Results were presented in Fig. 25d.

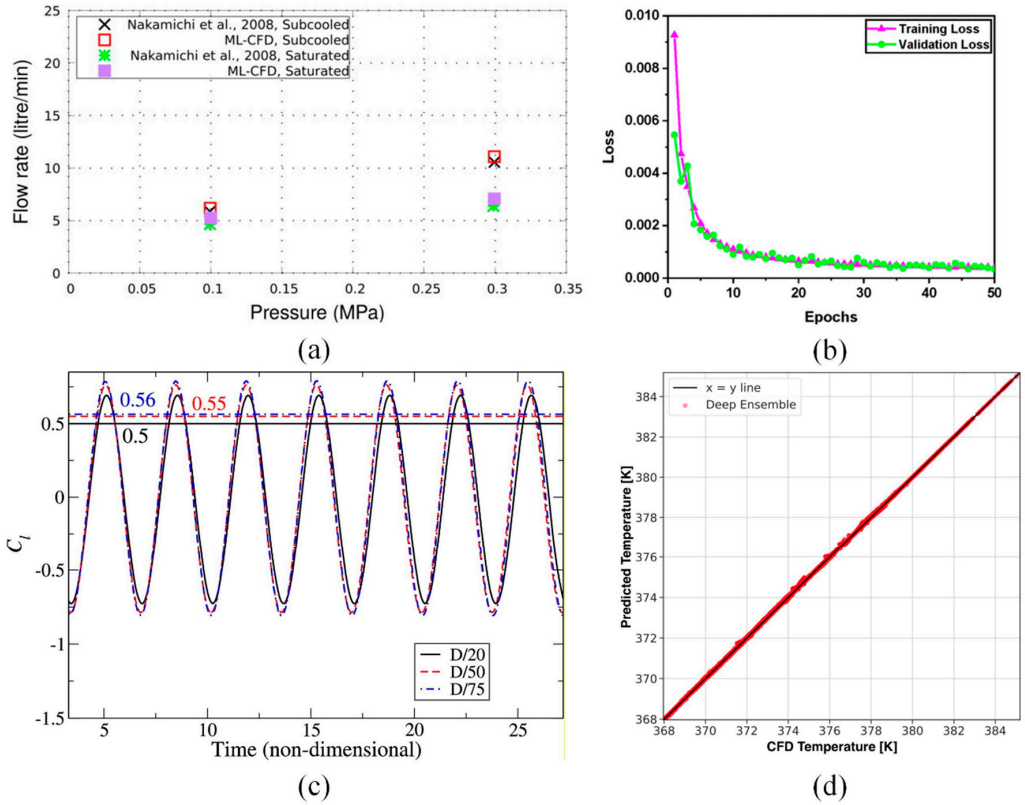

Figure 25: (**a**) Comparison of CFD and ML predictions with experimental measurements from Nakamichi et al. Reprinted from [109] (CC BY 4.0); (**b**) Training and validation loss versus epochs for the CFD-DNN model. Reprinted with permission from [110]. Copyright 2024, American Chemical Society; (**c**) Grid independence study for DRL-CFD. Reprinted with permission from [111]. Copyright 2024, Elsevier; (**d**) Validation Temperature regression chart of the computational domain. Adapted from [112] (CC BY 4.0).

In summary, DL-based methods enhance numerical simulation through specialized pathways. PINNs establish a physics-consistent solving paradigm that requires only boundary conditions to infer flow variable, excelling in flow reconstruction and complex phenomenon modeling where physical constraints are paramount [107,108]. In parallel, other DL approaches—including surrogate CNNs [109], CFD-DNN couplings [110], and DG-DRL-CFD method [111]—provide substantial gains in computational efficiency, serving as rapid surrogates for conventional solvers or optimizing entire CFD workflows. A common frontier for all these methods is the need for robust generalization and uncertainty quantification across diverse operating conditions [112]. The development of ultra-fast DL surrogates and PINNs is key for dynamic system analysis and online monitoring. Embedding these lightweight models allows for continuous generation of real-time performance data, which is essential for implementing advanced, model-based predictive control in complex industrial boilers or heat exchangers.

The AI-assisted numerical methods reviewed above offer distinct trade-offs. Physics-informed neural networks (PINNs) [107,108] embed governing equations into the loss function, ensuring physical consistency even with limited data—ideal for inverse problems or scenarios where physics is well understood but data is scarce. However, they can be computationally intensive to train. In contrast, purely data-driven surrogates (e.g., CFD-DNN [110], MLP-based models [104]) learn directly from simulation data and deliver orders-of-magnitude speed-up once trained, making them well-suited for design optimization or real-time control. Their main limitation is generalizability: predictions may become unreliable outside the training data range. Hybrid frameworks like DG-DRL-CFD [111] strike a balance, retaining physical fidelity while accelerating optimization in complex geometries. The choice thus depends on the research goal: high-fidelity physics exploration favors PINNs; rapid iterative evaluations favor data-driven surrogates; and control optimization may benefit from hybrid approaches.

Beyond these trade-offs, a broader paradigm shift is worth emphasizing: the move toward physics-informed and hybrid modeling reflects a growing recognition that for thermal science applications, models must be judged not only by accuracy but also by physical consistency and interpretability. PINNs offer the additional capability of inverse problems—inferring unknown parameters such as contact resistance or nucleation site density directly from experimental observations [107,108]. Hybrid mechanistic–data-driven approaches retain the interpretability of a physically grounded baseline while learning corrections for residual complexities. Meanwhile, interpretability techniques are advancing beyond post-hoc explanations (SHAP, LIME) toward architectures with inherent interpretability, such as attention mechanisms [60] or symbolic regression that distills learned relationships into explicit mathematical expressions. For the thermal science community—where physical insight is as valued as predictive power—these developments offer the promise of AI models that not only predict but also explain, serving as true partners in scientific discovery.

5.3 Synthesis: Mapping Studies to the Tri-Phase Framework

Looking across the studies reviewed in Sections 3–5, a clear evolutionary trajectory emerges in how AI has been applied to boiling heat transfer research. The field began with foundational models that established the feasibility of data-driven approaches—SVM and ANN for CHF/HTC prediction [38,63,70,71], and U-Net or Mask R-CNN for bubble segmentation [78,80–82]—demonstrating that machine learning could meaningfully address boiling problems. Building on these baselines, a second wave of methodological innovations introduced architectures tailored to domain-specific challenges: Transformers and hybrid DNN-XAI models achieving superior prediction accuracy [60,65–67], PINNs embedding physical constraints directly into simulations [107,108], and proposals for GNNs or 3D CNNs to explicitly model overlapping

bubble dynamics. Most recently, a third phase focused on industrial adaptation has begun to emerge, with soft sensors enabling real-time boiling point monitoring [59,102,103], DRL-CFD frameworks for active flow control [111], and an evolving synergy between AI-driven analysis and advanced surface engineering. This progression—from proof-of-concept, through methodological refinement, toward practical deployment—reflects a maturing field increasingly capable of translating AI advances into tangible thermal management solutions.

6 Conclusions and Perspectives

This paper systematically reviews recent advances in AI applications for boiling heat transfer research, focusing on these key aspects: intelligent prediction of boiling heat transfer parameters, bubble dynamics image recognition and parameter detection, soft sensor optimization, and numerical simulation enhancement. By synthesizing research findings from numerous scholars, we comprehensively summarize cutting-edge AI developments in this field, providing valuable references and insights. The main conclusions are as follows:

i. AI has demonstrated exceptional performance in predicting CHF and HTC, showing broader applicability, higher accuracy, and smaller errors compared to traditional empirical correlations. For boiling curve prediction, multi-model coupling or incorporation of morphological parameters yields more accurate and generalizable results.
ii. In bubble dynamics research, AI technologies exhibit remarkable advantages in image recognition, segmentation, and parameter quantification, significantly outperforming conventional methods in both precision and efficiency while demonstrating superior reliability compared to manual processing, thereby providing more powerful analytical tools.
iii. AI shows outstanding capabilities in soft sensor development and numerical simulation optimization, featuring zero-shot learning ability and substantially improved efficiency over traditional methods and early AI models, with dramatically reduced computation time, offering efficient technical solutions for complex heat transfer problems.

To provide a clear overview of the AI methods' application distribution and frequency, Table 7 categorizes the primary AI techniques based on their application areas and prevalence in boiling heat transfer research.

Table 7: AI Methods Application Frequency Matrix.

Application Domain	AI Method	Frequency	Representative Case
Boiling Curve Prediction	ANN/DNN	High	CHF prediction
	Transformer	High	HTC prediction
	Hybrid models	Medium	Boiling curve prediction
Bubble recognition	CNN	Very High	Bubble segmentation
	SVM	Low	Flow pattern ID
Bubble Dynamics Analysis	ANN, SD + U-Net	Medium	Nucleation parameters
	ANN, Mask R-CNN	Medium	Growth parameters
	XGBoost, ANN	Medium	Detachment parameters
Soft sensors	LSTM, SAE	Low	Boiling point measurement
Numerical methods	ANN, DL	Medium	Simulation optimization

This review of the literature reveals that the development of AI models in boiling heat transfer relies on a well-established ecosystem of data sources. These can be broadly categorized into experimental measurements, numerically generated data from high-fidelity CFD simulations, and extracted bubble

dynamics parameters. The scale of these datasets typically ranges from hundreds of data points for scalar parameter prediction to thousands of images or field data points for segmentation and surrogate modeling tasks. This diversity and maturity of data foundations underpin the robust progress in the field.

Current research has conclusively demonstrated the tremendous potential of AI in boiling heat transfer studies. To transition these advancements from laboratory proof-of-concept to robust industrial deployment, future research should prioritize the following interconnected frontiers:

i. Multiscale and Multiphysics Modeling: Applying AI to boiling heat transfer under more complex conditions to address challenges from strongly coupled multi-physics fields. This includes developing frameworks that seamlessly integrate pore-scale bubble nucleation with component-scale thermal performance, ultimately enabling system-level digital twins. A promising architecture is the graph network simulator [24–26], where bubbles are represented as nodes and their interactions as edges. Such a graph neural network (GNN) can learn bubble-scale dynamics and then be embedded within a larger finite element model of a heat sink, creating a truly integrated multiscale simulation framework.

ii. Overcoming the Data Bottleneck: A fundamental challenge is the scarcity and quality of experimental data—measurements are costly, and manual annotation of bubble images is error-prone. Addressing this requires a multi-pronged strategy. Transfer learning enables knowledge to be adapted across configurations with minimal data. Few-shot learning excels at learning from very limited examples. Synthetic data from high-fidelity simulations can provide unlimited, perfectly annotated training samples. Integrating these strategies offers a pathway toward robust, generalizable models unconstrained by limited experimental measurements.

iii. Embedded AI for Real-time Industrial Control: Developing lightweight, robust AI models for deployment on edge AI processors that can perform inference directly at the sensor location without cloud connectivity. Achieving this requires model compression techniques such as pruning (removing redundant neurons), quantization (reducing numerical precision from 32-bit to 8-bit or lower), and knowledge distillation (training compact student networks to mimic larger teacher models). These techniques can reduce model size and latency by an order of magnitude while maintaining acceptable accuracy, enabling real-time applications such as vision-based boiling regime identification for early dryout warning, or ultra-fast surrogate models for model-predictive control in industrial heat exchangers.

iv. Enhancing Reliability and Trust: Future work must emphasize model interpretability and uncertainty quantification (UQ). Techniques like SHAP and LIME can reveal physical insights from black-box models. For UQ, methods such as Monte Carlo Dropout, deep ensembles, and Bayesian neural networks can quantify prediction confidence by generating uncertainty estimates alongside predictions. In digital twin frameworks for boiling systems, integrating these UQ techniques enables real-time confidence intervals and flags when predictions become unreliable—transforming AI from a black-box predictor into a trustworthy component for safety-critical thermal management.

v. Establishing Ground Physical Validation: The issue of physical truth reliability in bubble identification—exemplified by the challenges of manual counting at high heat flux densities discussed in *Instance Segmentation with Mask R-CNN and Alternatives*—underscores the need for more robust validation frameworks. Future work should complement human annotations with synthetic datasets, cross-validation against physically consistent simulations, or evaluation based on downstream physical quantities (e.g., heat transfer coefficients) that are less sensitive to individual counting errors.

Finally, it is worth emphasizing that the AI methods reviewed herein are not merely analytical tools—they can form a powerful synergy with cutting-edge experimental surface engineering. Recent

studies have demonstrated remarkable boiling enhancements through sophisticated surface architectures, such as 3D cage-engineered biphilic surfaces [113] and hybrid dividing zones of micro-nano structures [114]. These designs achieve simultaneous improvements in ONB, HTC, and CHF through complex, multi-scale surface features. The AI techniques reviewed in this paper—particularly CNNs for bubble dynamics characterization [80,84] and hybrid models for CHF prediction [66,67]—are ideally suited to analyze the intricate bubble behaviors on such novel surfaces and to guide their optimization. This creates a powerful feedback loop: advanced surface engineering generates rich physical phenomena, and AI-powered analysis extracts the mechanistic insights needed to inform the next generation of surface designs.

These breakthroughs will open new frontiers in boiling heat transfer research, driving the field toward intelligent and precise development.

Acknowledgement: The authors acknowledge the support of their respective institutions.

Funding Statement: This work was supported by the Postgraduate Research & Practice Innovation Program of Jiangsu Province [grant number KYCX23_3697].

Author Contributions: Wei-Chen Tang was responsible for study conception, literature analysis, and manuscript preparation. Xin Chen and Fei Dong contributed to manuscript review, critical revision, and supervision. Fei Dong secured funding and oversaw the project. All authors reviewed and approved the final version of the manuscript.

Availability of Data and Materials: This review article does not involve the generation of new experimental or simulation data. All data discussed in this manuscript are derived from previously published sources, which are appropriately cited within the text and listed in the references section.

Ethics Approval: Not applicable.

Conflicts of Interest: The authors declare no conflicts of interest.

References

1. Sajjad U, Hussain I, Hamid K, Ali HM, Wang CC, Yan WM. Liquid-to-vapor phase change heat transfer evaluation and parameter sensitivity analysis of nanoporous surface coatings. Int J Heat Mass Transf. 2022;194:123088. [CrossRef].
2. Ali MR, Al-Khaled K, Hussain M, Labidi T, Khan SU, Kolsi L, et al. Effect of design parameters on passive control of heat transfer enhancement phenomenon in heat exchangers—A brief review. Case Stud Therm Eng. 2023;43:102674. [CrossRef].
3. Wang Y, Wu G, Xu J, Chen R, Wang H. Effects of geometric arrangement on pool boiling heat exchange in the tubular bundle. Nucl Eng Des. 2023;402:112110. [CrossRef].
4. Zhang Y, Ma X, Zhu Z, Duan L, Wei J. Critical heat flux prediction model of pool boiling heat transfer on the micro-pillar surfaces. Case Stud Therm Eng. 2021;28:101668. [CrossRef].
5. Liang G, Mudawar I. Review of pool boiling enhancement by surface modification. Int J Heat Mass Transf. 2019;128:892–933. [CrossRef].
6. Huang M, Borzoei H, Abdollahi A, Li Z, Karimipour A. Effect of concentration and sedimentation on boiling heat transfer coefficient of GNPs-SiO_2/deionized water hybrid Nanofluid: An experimental investigation. Int Commun Heat Mass Transf. 2021;122:105141. [CrossRef].
7. Oikonomidou O, Evgenidis S, Argyropoulos C, Zabulis X, Karamaoynas P, Raza MQ, et al. Bubble growth analysis during subcooled boiling experiments on-board the international space station: Benchmark image analysis. Adv Colloid Interface Sci. 2022;308:102751. [CrossRef].
8. Poletaev I, Tokarev MP, Pervunin KS. Bubble patterns recognition using neural networks: Application to the analysis of a two-phase bubbly jet. Int J Multiph Flow. 2020;126:103194. [CrossRef].

9. Saha K, Kumar Agarwal A, Ghosh K, Som S. Two-phase flow for automotive and power generation sectors. Singapore: Springer; 2019. [CrossRef].
10. Shi L, Yang Y, Zhao G, Liu P, Zhao D, Qin F, et al. Research and development on inlets for rocket based combined cycle engines. Prog Aerosp Sci. 2020;117:100639. [CrossRef].
11. Roy A, Chakraborty S. Support vector machine in structural reliability analysis: A review. Reliab Eng Syst Saf. 2023;233:109126. [CrossRef].
12. Du KL, Jiang B, Lu J, Hua J, Swamy MNS. Exploring kernel machines and support vector machines: Principles, techniques, and future directions. Mathematics. 2024;12(24):3935. [CrossRef].
13. Tychola KA, Kalampokas T, Papakostas GA. Quantum machine learning—An overview. Electronics. 2023;12(11):2379. [CrossRef].
14. Foukalas F. A survey of artificial neural network computing systems. Cogn Comput. 2024;17(1):4. [CrossRef].
15. Iskhakov AS, Dinh NT, Chen E. Integration of neural networks with numerical solution of PDEs for closure models development. Phys Lett A. 2021;406:127456. [CrossRef].
16. Schmidgall S, Ziaei R, Achterberg J, Kirsch L, Hajiseyedrazi SP, Eshraghian J. Brain-inspired learning in artificial neural networks: A review. APL Mach Learn. 2024;2(2):021501. [CrossRef].
17. Gallego AJ, Calvo-Zaragoza J, Valero-Mas JJ, Rico-Juan JR. Clustering-based k-nearest neighbor classification for large-scale data with neural codes representation. Pattern Recognit. 2018;74:531–43. [CrossRef].
18. Ukey N, Yang Z, Li B, Zhang G, Hu Y, Zhang W. Survey on exact kNN queries over high-dimensional data space. Sensors. 2023;23(2):629. [CrossRef].
19. Lu HM, Chen JS, Liao WC. Nonparametric regression *via* variance-adjusted gradient boosting Gaussian process regression. IEEE Trans Knowl Data Eng. 2021;33(6):2669–79. [CrossRef].
20. Chen MH, Yu CH, Gao JL, Yu K, Lin S, Guo GD, et al. Quantum algorithm for Gaussian process regression. Phys Rev A. 2022;106:012406. [CrossRef].
21. Valueva MV, Nagornov NN, Lyakhov PA, Valuev GV, Chervyakov NI. Application of the residue number system to reduce hardware costs of the convolutional neural network implementation. Math Comput Simul. 2020;177:232–43. [CrossRef].
22. Tian Y. Artificial intelligence image recognition method based on convolutional neural network algorithm. IEEE Access. 2020;8:125731–44. [CrossRef].
23. Bera S, Shrivastava VK, Chandra Satapathy S. Advances in hyperspectral image classification based on convolutional neural networks: A review. Comput Model Eng Sci. 2022;133(2):219–50. [CrossRef].
24. Sharma A, Singh S, Ratna S. Graph neural network operators: A review. Multimed Tools Appl. 2024;83(8):23413–36. [CrossRef].
25. Feng G, Wang H, Wang C. Search for deep graph neural networks. Inf Sci. 2023;649:119617. [CrossRef].
26. Lin H, Yan M, Ye X, Fan D, Pan S, Chen W, et al. A comprehensive survey on distributed training of graph neural networks. Proc IEEE. 2023;111(12):1572–606. [CrossRef].
27. Mei D, Zhou K, Liu CH. Unified finite-volume physics informed neural networks to solve the heterogeneous partial differential equations. Knowl Based Syst. 2024;295:111831. [CrossRef].
28. Zhang ZY, Zhang H, Liu Y, Li JY, Liu CB. Generalized conditional symmetry enhanced physics-informed neural network and application to the forward and inverse problems of nonlinear diffusion equations. Chaos Solitons Fractals. 2023;168:113169. [CrossRef].
29. Ryu I, Park GB, Lee Y, Choi DH. Physics-informed neural network for engineers: A review from an implementation aspect. J Mech Sci Technol. 2024;38(7):3499–519. [CrossRef].
30. Rhodes JS, Cutler A, Moon KR. Geometry- and accuracy-preserving random forest proximities. IEEE Trans Pattern Anal Mach Intell. 2023;45(9):10947–59. [CrossRef].
31. Ghosh D, Cabrera J. Enriched random forest for high dimensional genomic data. IEEE/ACM Trans Comput Biol Bioinform. 2022;19(5):2817–28. [CrossRef].
32. Oktavian MR, Nistor J, Gruenwald JT, Xu Y. Preliminary development of machine learning-based error correction model for low-fidelity reactor physics simulation. Ann Nucl Energy. 2023;187:109788. [CrossRef].
33. Noh H, Lee S, Kim SM, Mudawar I. Utilization of XGBoost algorithm to predict dryout incipience quality for saturated flow boiling in mini/micro-channels. Int J Heat Mass Transf. 2024;231:125827. [CrossRef].

34. Mersha M, Lam K, Wood J, AlShami AK, Kalita J. Explainable artificial intelligence: A survey of needs, techniques, applications, and future direction. Neurocomputing. 2024;599:128111. [CrossRef].
35. Liu G, Zhang J, Chan AB, Hsiao JH. Human attention guided explainable artificial intelligence for computer vision models. Neural Netw. 2024;177:106392. [CrossRef].
36. Chu H, Ji T, Yu X, Liu Z, Rui Z, Xu N. Advances in the application of machine learning to boiling heat transfer: A review. Int J Heat Fluid Flow. 2024;108:109477. [CrossRef].
37. Yang B, Zhu X, Wei B, Liu M, Li Y, Lv Z, et al. Computer vision and machine learning methods for heat transfer and fluid flow in complex structural microchannels: A review. Energies. 2023;16(3):1500. [CrossRef].
38. Cabarcos A, Paz C, Suarez E, Vence J. Application of supervised learning algorithms for temperature prediction in nucleate flow boiling. Appl Therm Eng. 2024;240:122155. [CrossRef].
39. Le J, Yang M, Guo M, Tian Y, Zhang H. Progress and prospects of artificial intelligence development and applications in supersonic flow and combustion. Prog Aerosp Sci. 2024;151:101046. [CrossRef].
40. Cordeiro-Costas M, Villanueva D, Eguía-Oller P, Granada-Álvarez E. Machine learning and deep learning models applied to photovoltaic production forecasting. Appl Sci. 2022;12(17):8769. [CrossRef].
41. Sabzekar M, Hasheminejad SMH. Robust regression using support vector regressions. Chaos Solitons Fractals. 2021;144:110738. [CrossRef].
42. Martínez-Comesaña M, Febrero-Garrido L, Granada-Álvarez E, Martínez-Torres J, Martínez-Mariño S. Heat loss coefficient estimation applied to existing buildings through machine learning models. Appl Sci. 2020;10(24):8968. [CrossRef].
43. Ooi ZJ, Zhu L, Bottini JL, Brooks CS. Identification of flow regimes in boiling flows in a vertical annulus channel with machine learning techniques. Int J Heat Mass Transf. 2022;185:122439. [CrossRef].
44. Xie X. Regularized multi-view least squares twin support vector machines. Appl Intell. 2018;48(9):3108–15. [CrossRef].
45. Gendeel M, Zhang Y, Qian X, Xing Z. Deterministic and probabilistic interval prediction for wind farm based on VMD and weighted LS-SVM. Energy Sources Part A Recovery Util Environ Eff. 2021;43(7):800–14. [CrossRef].
46. Jaeger A, Banks D. Cluster analysis: A modern statistical review. Wires Comput Stat. 2023;15(3):e1597. [CrossRef].
47. Ikotun AM, Ezugwu AE, Abualigah L, Abuhaija B, Jia H. K-means clustering algorithms: A comprehensive review, variants analysis, and advances in the era of big data. Inf Sci. 2023;622:178–210. [CrossRef].
48. Cui W, Yang Y. Quantum simultaneous measurement of non-commuting observables based on K-means clustering. Phys A Stat Mech Appl. 2022;588:126559. [CrossRef].
49. Govender P, Sivakumar V. Application of k-means and hierarchical clustering techniques for analysis of air pollution: A review (1980–2019). Atmos Pollut Res. 2020;11(1):40–56. [CrossRef].
50. Pearson K. LIII. On lines and planes of closest fit to systems of points in space. Lond Edinb Dublin Philos Mag J Sci. 1901;2(11):559–72. [CrossRef].
51. Beardslee L, Shokouhi P, Ulrich TJ. Optimal measurement point selection for resonant ultrasound spectroscopy of complex-shaped specimens using principal component analysis. NDT E Int. 2024;141:103000. [CrossRef].
52. Ahmed M, Habib A, Nawal MM, Saikot MMH, Chowdhury MAH, Hoque MA, et al. Deep learning-based approach to R-134a bubble detection and analysis for geothermal applications. Case Stud Therm Eng. 2023;49:103377. [CrossRef].
53. Rokoni A, Zhang L, Soori T, Hu H, Wu T, Sun Y. Learning new physical descriptors from reduced-order analysis of bubble dynamics in boiling heat transfer. Int J Heat Mass Transf. 2022;186:122501. [CrossRef].
54. Radaideh MI, Forget B, Shirvan K. Large-scale design optimisation of boiling water reactor bundles with neuroevolution. Ann Nucl Energy. 2021;160:108355. [CrossRef].
55. Ghazvini M, Varedi-Koulaei S, Ahmadi M, Kim M. Optimization of MLP neural network for modeling flow boiling performance of Al_2O_3/water nanofluids in a horizontal tube. Eng Anal Bound Elem. 2022;145:363–95. [CrossRef].
56. Cerqueira RFL, Paladino EE. Development of a deep learning-based image processing technique for bubble pattern recognition and shape reconstruction in dense bubbly flows. Chem Eng Sci. 2021;230:116163. [CrossRef].
57. Yuan X, Li L, Wang Y. Nonlinear dynamic soft sensor modeling with supervised long short-term memory network. IEEE Trans Ind Inform. 2020;16(5):3168–76. [CrossRef].

58. Yuan X, Li L, Wang Y, Yang C, Gui W. Deep learning for quality prediction of nonlinear dynamic processes with variable attention-based long short-term memory network. Can J Chem Eng. 2020;98(6):1377–89. [CrossRef].
59. Yuan X, Li L, Shardt YAW, Wang Y, Yang C. Deep learning with spatiotemporal attention-based LSTM for industrial soft sensor model development. IEEE Trans Ind Electron. 2021;68(5):4404–14. [CrossRef].
60. Zhou W, Miwa S, Wang H, Okamoto K. Assessment of the state-of-the-art AI methods for critical heat flux prediction. Int Commun Heat Mass Transf. 2024;158:107844. [CrossRef].
61. Mehdi S, Borumand M, Hwang G. Accurate and robust predictions of pool boiling heat transfer with micro-structured surfaces using probabilistic machine learning models. Int J Heat Mass Transf. 2024;226:125487. [CrossRef].
62. Soffer Y, Aharon Y, Ziskind G. Experimental investigation on incipient boiling in narrow closed gaps with water. Int J Therm Sci. 2023;191:108333. [CrossRef].
63. Kumar V, Pimparkar D, Saini VR, Kohli R, Gupta S, Pothukuchi H. Prediction of CHF location through applied machine learning. Prog Nucl Energy. 2024;169:105055. [CrossRef].
64. Becker KM, Ling CH, Hedberg S, Strand G. An experimental investigation of post dryout heat transfer. Stockholm, Sweden: Royal Institute of Technology; 1983.
65. Wang K, Wang D, Liu X, Cheng S, Wang S, Zhou W, et al. Re-examining the input-parameters and AI strategies for Critical Heat Flux prediction. Energy. 2025;318:134606. [CrossRef].
66. Zubair Khalid R, Ahmed I, Ullah A, Zio E, Khan A. Enhancing accuracy of prediction of critical heat flux in Circular channels by ensemble of deep sparse autoencoders and deep neural Networks. Nucl Eng Des. 2024;429:113587. [CrossRef].
67. Sajjad U, Mehdi S, Hussain I, Rehman TU, Sultan M, Rashidi MM, et al. Physics driven interpretable deep learning-based insights into boiling crisis of smooth and roughened surfaces. Alex Eng J. 2025;116:112–28. [CrossRef].
68. Mondal A, Kim NH. Nucleate pool boiling of R-134a on enhanced horizontal surfaces having pores on sub-tunnels. J Enh Heat Transf. 2019;26(3):195–216. [CrossRef].
69. Mehdi S, Shah Y, Mondal A, Kim NH. Bubble dynamics of R-134a boiling in enhanced surfaces having pores on sub-tunnels. Int J Heat Mass Transf. 2020;155:119753. [CrossRef].
70. Sajjad U, Raza W, Hussain I, Sultan M, Ali HM, Rubab N, et al. On the prediction and optimization of the flow boiling heat transfer in mini and micro channel heat sinks. Prog Nucl Energy. 2024;177:105466. [CrossRef].
71. Ayoobi A, Khorasani AF, Barzegar M, Zavare MHN. Experimental study on the effects of water hardness during transient pool boiling and the development of an artificial neural network. Int J Heat Mass Transf. 2024;227:125563. [CrossRef].
72. Mehdi S, Nannapaneni S, Hwang G. Structural-material-operational performance relationship for pool boiling on enhanced surfaces using deep neural network model. Int J Heat Mass Transf. 2022;198:123395. [CrossRef].
73. Sajjad U, Hussain I, Imran M, Sultan M, Wang CC, Alsubaie AS, et al. Boiling heat transfer evaluation in nanoporous surface coatings. Nanomaterials. 2021;11(12):3383. [CrossRef].
74. Sajjad U, Hussain I, Wang CC. A high-fidelity approach to correlate the nucleate pool boiling data of roughened surfaces. Int J Multiph Flow. 2021;142:103719. [CrossRef].
75. Sajjad U, Yan WM, Hussain I, Mehdi S, Sultan M, Ali HM, et al. Physics and correlations informed deep learning to foresee various regimes of the pool boiling curve. Eng Appl Artif Intell. 2024;136:108867. [CrossRef].
76. Scariot VK, Hobold GM, da Silva AK. Data-driven diagnostics of boiling heat transfer on flat heaters from non-intrusive visualization. Appl Therm Eng. 2024;248:123068. [CrossRef].
77. Suh Y, Bostanabad R, Won Y. Deep learning predicts boiling heat transfer. Sci Rep. 2021;11:5622. [CrossRef].
78. Ravichandran M, Kossolapov A, Aguiar GM, Phillips B, Bucci M. Autonomous and online detection of dry areas on a boiling surface using deep learning and infrared thermometry. Exp Therm Fluid Sci. 2023;145:110879. [CrossRef].
79. Hessenkemper H, Starke S, Atassi Y, Ziegenhein T, Lucas D. Bubble identification from images with machine learning methods. Int J Multiph Flow. 2022;155:104169. [CrossRef].
80. Malakhov I, Seredkin A, Chernyavskiy A, Serdyukov V, Mullyadzanov R, Surtaev A. Deep learning segmentation to analyze bubble dynamics and heat transfer during boiling at various pressures. Int J Multiph Flow. 2023;162:104402. [CrossRef].

81. Dunlap C, Li C, Pandey H, Le N, Hu H. BubbleID: A deep learning framework for bubble interface dynamics analysis. J Appl Phys. 2024;136:014902. [CrossRef].
82. Schepperle M, Junaid S, Woias P. Computer-vision- and deep-learning-based determination of flow regimes, void fraction, and resistance sensor data in microchannel flow boiling. Sensors. 2024;24(11):3363. [CrossRef].
83. Seong JH, Ravichandran M, Su G, Phillips B, Bucci M. Automated bubble analysis of high-speed subcooled flow boiling images using U-Net transfer learning and global optical flow. Int J Multiph Flow. 2023;159:104336. [CrossRef].
84. Kang Q, Ye F, Li Q, Li R, Wang J, Wang H, et al. Bubble boundary R-CNN: A multitask model for segmenting and reconstructing overlapping bubbles. Sep Purif Technol. 2025;358:130300. [CrossRef].
85. Haas T, Schubert C, Eickhoff M, Pfeifer H. BubCNN: Bubble detection using Faster RCNN and shape regression network. Chem Eng Sci. 2020;216:115467. [CrossRef].
86. Soibam J, Scheiff V, Aslanidou I, Kyprianidis K, Bel Fdhila R. Application of deep learning for segmentation of bubble dynamics in subcooled boiling. Int J Multiph Flow. 2023;169:104589. [CrossRef].
87. Zhu L, Xiao X, Wu D, Wang Y, Qing X, Xue W. Qualitative classification of lubricating oil wear particle morphology based on coaxial capacitive sensing network and SVM. Sensors. 2022;22(17):6653. [CrossRef].
88. Carvalho V, Gonçalves IM, Souza A, Souza MS, Bento D, Ribeiro JE, et al. Manual and automatic image analysis segmentation methods for blood flow studies in microchannels. Micromachines. 2021;12(3):317. [CrossRef].
89. Chen X, Liang H, Li Y, Chen D, Wang J, Chen J. Development of an imaging and impedance flow cytometer based on a constriction microchannel and deep neural pattern recognition. IEEE Trans Electron Devices. 2022;69(11):6408–16. [CrossRef].
90. Roshani M, Phan GTT, Jammal Muhammad Ali P, Hossein Roshani G, Hanus R, Duong T, et al. Evaluation of flow pattern recognition and void fraction measurement in two phase flow independent of oil pipeline's scale layer thickness. Alex Eng J. 2021;60(1):1955–66. [CrossRef].
91. Sestito GS, Álvarez-Briceño R, Ribatski G, da Silva MM, de Oliveira LPR. Vibration-based multiphase-flow pattern classification *via* machine learning techniques. Flow Meas Instrum. 2023;89:102290. [CrossRef].
92. Schmidt U, Weigert M, Broaddus C, Myers G. Cell detection with star-convex polygons. In: Proceedings of the Medical Image Computing and Computer Assisted Intervention—MICCAI 2018; 2018 Sep 16–20; Granada, Spain. p. 265–73. [CrossRef].
93. Zhao Y, Wang Z, Liu Q, Wu Y, Lyu J. Bubble behavior parameters extraction and analysis during pool boiling based on deep-learning method. Int J Multiph Flow. 2024;180:104979. [CrossRef].
94. Rassoulinejad-Mousavi SM, Al-Hindawi F, Soori T, Rokoni A, Yoon H, Hu H, et al. Deep learning strategies for critical heat flux detection in pool boiling. Appl Therm Eng. 2021;190:116849. [CrossRef].
95. Mohanty RL, Das MK. A critical review on bubble dynamics parameters influencing boiling heat transfer. Renew Sustain Energy Rev. 2017;78:466–94. [CrossRef].
96. Eskandari E, Alimoradi H, Pourbagian M, Shams M. Numerical investigation and deep learning-based prediction of heat transfer characteristics and bubble dynamics of subcooled flow boiling in a vertical tube. Korean J Chem Eng. 2022;39(12):3227–45. [CrossRef].
97. Moiz M, Prajapat R, Srivastava A, Srivastava A. Machine learning-inspired study of dynamical parameters of single vapor bubble under nucleate flow boiling regime. Appl Therm Eng. 2025;259:124827. [CrossRef].
98. Moiz M, Prajapat R, Srivastava A. Prediction of bubble dynamics parameters in nucleate flow boiling using artificial neural networks (ANN). Int Commun Heat Mass Transf. 2025;162:108668. [CrossRef].
99. Deng K, Tan B, Cheng S, Sun R, Ren H. Investigating bubble dynamics on silicon carbide surfaces during flow boiling. Case Stud Therm Eng. 2024;60:104807. [CrossRef].
100. Ali Alavi Fazel S. Prediction of bubble departing diameter in pool boiling of mixtures by ANN using modified ReLU. Heliyon. 2024;10(11):e31261. [CrossRef].
101. He Y, Hu C, Li H, Hu X, Tang D. Reliable predictions of bubble departure frequency in subcooled flow boiling: A machine learning-based approach. Int J Heat Mass Transf. 2022;195:123217. [CrossRef].
102. Yuan X, Feng L, Wang K, Wang Y, Ye L. Deep learning for data modeling of multirate quality variables in industrial processes. IEEE Trans Instrum Meas. 2021;70:2509611. [CrossRef].

103. Yuan X, Ou C, Wang Y, Yang C, Gui W. A layer-wise data augmentation strategy for deep learning networks and its soft sensor application in an industrial hydrocracking process. IEEE Trans Neural Netw Learn Syst. 2021;32(8):3296–305. [CrossRef].
104. Fallahtafti N, Hosseini F, Hadad Y, Rangarajan S, Hoang CH, Sammakia B. Experimental characterization and geometrical optimization of a commercial two-phase designed cold plate. Int Commun Heat Mass Transf. 2024;155:107457. [CrossRef].
105. Cai S, Mao Z, Wang Z, Yin M, Karniadakis GE. Physics-informed neural networks (PINNs) for fluid mechanics: A review. Acta Mech Sin. 2021;37(12):1727–38. [CrossRef].
106. Fernández de la Mata F, Gijón A, Molina-Solana M, Gómez-Romero J. Physics-informed neural networks for data-driven simulation: Advantages, limitations, and opportunities. Phys A Stat Mech Appl. 2023;610:128415. [CrossRef].
107. M Silva R, Grave M, Coutinho ALGA. A PINN-based level-set formulation for reconstruction of bubble dynamics. Arch Appl Mech. 2024;94(9):2667–82. [CrossRef].
108. Jalili D, Mahmoudi Y. Physics-informed neural networks for two-phase film boiling heat transfer. Int J Heat Mass Transf. 2025;241:126680. [CrossRef].
109. Bhatia D, Loukas J, Cabrera A, Lyras K. A deep learning computational fluid dynamics solver for simulating liquid hydrogen jets. Phys Fluids. 2024;36(5):057120. [CrossRef].
110. Dhakane V, Yadav A. Computational fluid dynamics–deep neural network (CFD-DNN) surrogate model with graphical user interface (GUI) for predicting hydrodynamic parameters in three-phase bubble column reactors. Ind Eng Chem Res. 2024;63(26):11670–85. [CrossRef].
111. Raut HS, Bhattacharya A, Sharma A. A dual grid-based deep reinforcement learning and computational fluid dynamics method for flow control and its application to nucleate pool boiling. Int J Heat Mass Transf. 2024;227:125561. [CrossRef].
112. Soibam J, Rabhi A, Aslanidou I, Kyprianidis K, Bel Fdhila R. Derivation and uncertainty quantification of a data-driven subcooled boiling model. Energies. 2020;13(22):5987. [CrossRef].
113. Wang S, Fan B, Yang X, Xie S, Jiang X. Three-dimensional cage-engineered biphilic surfaces controlling thermal-fluidic interactions for boiling enhancement. Phys Fluids. 2025;37(12):122023. [CrossRef].
114. Jiang X, Ali Shah SW, Chen G, Xie S. Extraordinary boiling enhancement by hybrid dividing zones of micro-nano structures. Int Commun Heat Mass Transf. 2024;153:107345. [CrossRef].